Fall 2008

Modeling, analysis and experimentation for building ice parts with supports using rapid freeze prototyping

Frances D. Bryant

Department: Mechanical and Aerospace Engineering

MODELING, ANALYSIS AND EXPERIMENTATION FOR BUILDING ICE PARTS WITH SUPPORTS USING RAPID FREEZE PROTOTYPING

by

FRANCES DENISE BRYANT

A DISSERTATION

Presented to the Faculty of the Graduate School of the

MISSOURI UNIVERSITY OF SCIENCE AND TECHNOLOGY

In Partial Fulfillment of the Requirements for the Degree

DOCTOR OF PHILOSOPHY

in

MECHANICAL ENGINEERING

2008

Approved by:

Ming Leu, Advisor
Frank Liou
Robert Landers
Gary Bertrand
Greg Hilmas

ABSTRACT

Rapid Freeze Prototyping (RFP) is a freeform fabrication method that freezes water droplets into ice in a layer-by-layer manner to additively create a 3-dimensional part. Each layer of a geometry is deposited and allowed to freeze before the next layer is added. Ice parts produced by RFP can be used in investment casting to replace wax patterns and in other applications which may benefit from the unconventional method of using ice as a pattern or mold. More recently, a sacrificial support material has been incorporated into RFP so that over-hung areas and complex geometries can be fabricated.

The research presented in this PhD dissertation study intends to provide information about a selected support material that has been implemented into the RFP process. The work first presents an overview of the process parameters of the system and the effects they have on the overall build dimensions and surface finish. The work continues on to the investigation process of finding a suitable support material to be used in conjunction with water/ice in RFP. The work then presents a model which illustrates the interaction occurring during fabrication of the main build material (i.e. water freezing to ice) and the support material. Two types of models are derived and explained, which are thermal and concentration models. These models are derived, described in detail, and their solutions obtained by finite element analysis are given. Experimentally obtained data is compared to predictions from the thermal and concentration models. Dimensional accuracy of finished ice parts is also examined for various build parameters. Measurements of geometric features of ice parts are presented as an indication of the dimensional accuracy build capability of RFP. Surface roughness measurements are also given. Sample ice parts are shown throughout the dissertation document.

ACKNOWLEDGMENTS

I would like to express my sincere gratitude to my advisor, Dr. Ming Leu for his guidance, advice and support throughout this study. I appreciate all the time he spent helping with this study and the advice he provided.

I would also like to acknowledge and thank my dissertation committee: Dr. Robert Landers and Dr. Frank Liou, from the Department of Mechanical and Aerospace Engineering; Dr. Gary Bertrand from the Department of Chemistry; and Dr. Greg Hilmas, from the Department of Materials Science and Engineering.

I would like to thank my fellow students working in the Virtual and Rapid Prototyping Laboratory.

Finally, I would like to thank the Department of Education, The National Science Foundation and the Department of Mechanical and Aerospace Engineering at the Missouri University of Science & Technology for providing funding throughout the course of this study.

TABLE OF CONTENTS

Page

LIST OF ILLUSTRATIONS

LIST OF TABLES

NOMENCLATURE

Symbol	Description
f	volumetric feed rate
v	scan speed
p	pressure
d	nozzle diameter
m	mass
σ	surface tension
V	volume
N	duty cycle
g	gravitational constant
Δh	height
A	area
t	time
Δz	layer thickness
w	line width
α	contact angle
R	surface roughness
I	area for surface roughness calculation
r_o	half line width
k	surface roughness coefficient
E	enthalpy
λ	thermal conductivity
T	temperature
b	$\frac{2h}{\lambda w}$
h	heat transfer coefficient
ϕ	thermal diffusivity
ρ	density
L	latent heat of fusion

c	specific heat
J	mass flux
D	diffusion coefficient
C	concentration
x,y	coordinates
q	internal heat generation
δ	new layer height

1. INTRODUCTION

Solid freeform fabrication (SFF), also known as Rapid Prototyping (RP), originated in the early 1980's. There are numerous types of RP available today, both commercially and in research labs around the world. Some of the well known RP methods include Stereolithography (SLA), Fused Deposition Modeling (FDM), Selective Laser Sintering (SLS), Laminated Object Manufacturing (LOM), Three-dimensional printing (3D-P), and Direct Metal Deposition (DMD). The build materials used in these various types of SFF methods vary with each type, but range from metal to paper to polymers. Each of these methods generally begins with a CAD model and utilizes a slicing program to create the geometry from very thin slices. The slice geometry is then used to build the three-dimensional part in a layer-by-layer manner. Some methods, such as SLA, SLS, LOM, and 3D-P, use the main build material for support when building complex parts. Other methods, such as FDM and DMD, however, use a completely different material as the support material. Methods of support removal vary within these techniques.

1.1 BACKGROUND AND PREVIOUS RELEVANT WORK

Rapid Freeze Prototyping (RFP) is a relatively new SFF technique. RFP is a method that uses water freezing into ice as its medium to create three-dimensional parts. Many types of SFF techniques use heat to deposit a material in an additive process to produce a physical part. RFP is a process that builds ice parts in a low-temperature environment by depositing and freezing water droplets layer by layer. By using a cooling method instead of a heating method to build parts, many advantages can be achieved by using RFP. Some of these advantages include having less expensive equipment and

material, a cleaner material and process, less energy consumption, better surface finish, and ease of building multi-color parts [Sui and Leu, 2003].

The RFP building process is conducted in a freezer. A drop-on-demand nozzle moves in a prescribed manner and deposits water, or support material, layer-by-layer at desired locations according to the cross-sections of the three-dimensional geometry. The setup also consists of a gravity-fed containment unit, an X-Y table to control the substrate to obtain the correct layer geometry, a Z-axis elevator to raise the nozzles for the successive layers, and two circuit driven nozzles. Figure 1.1 shows a schematic of the RFP setup used to conduct experiments and create ice parts in this dissertation work. Figure 1.2 shows a photograph of the equipment in the vicinity of the build area inside the freezer.

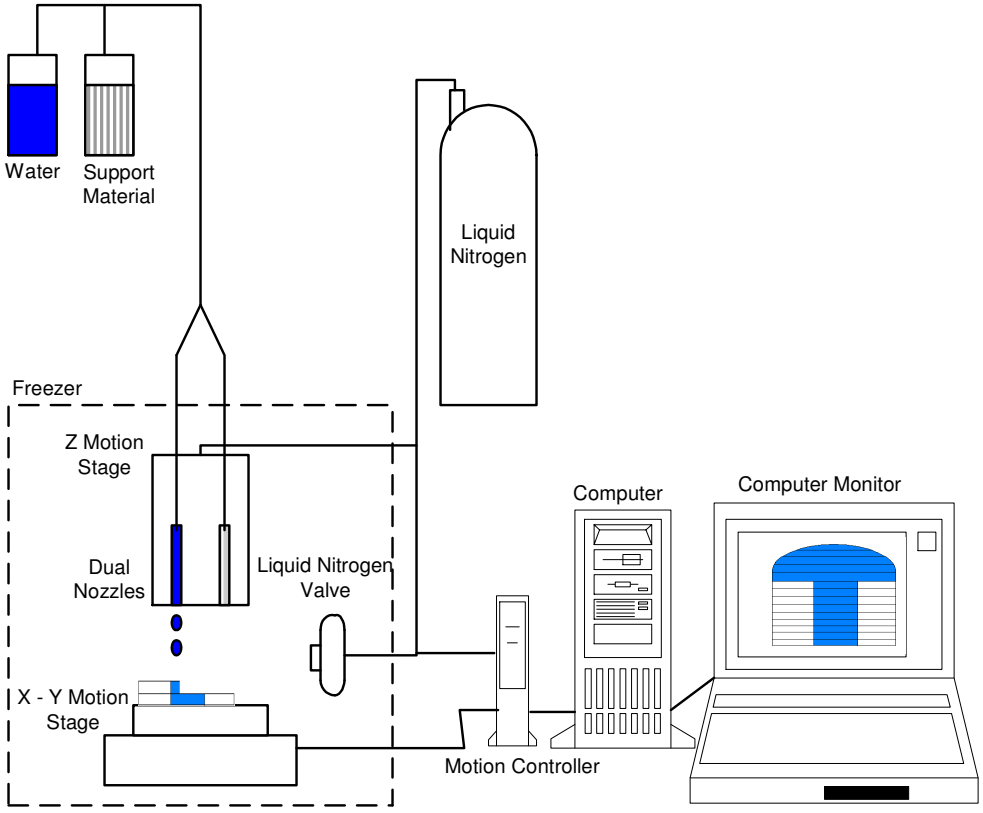

Figure 1.1. Principle of Rapid Freeze Prototyping

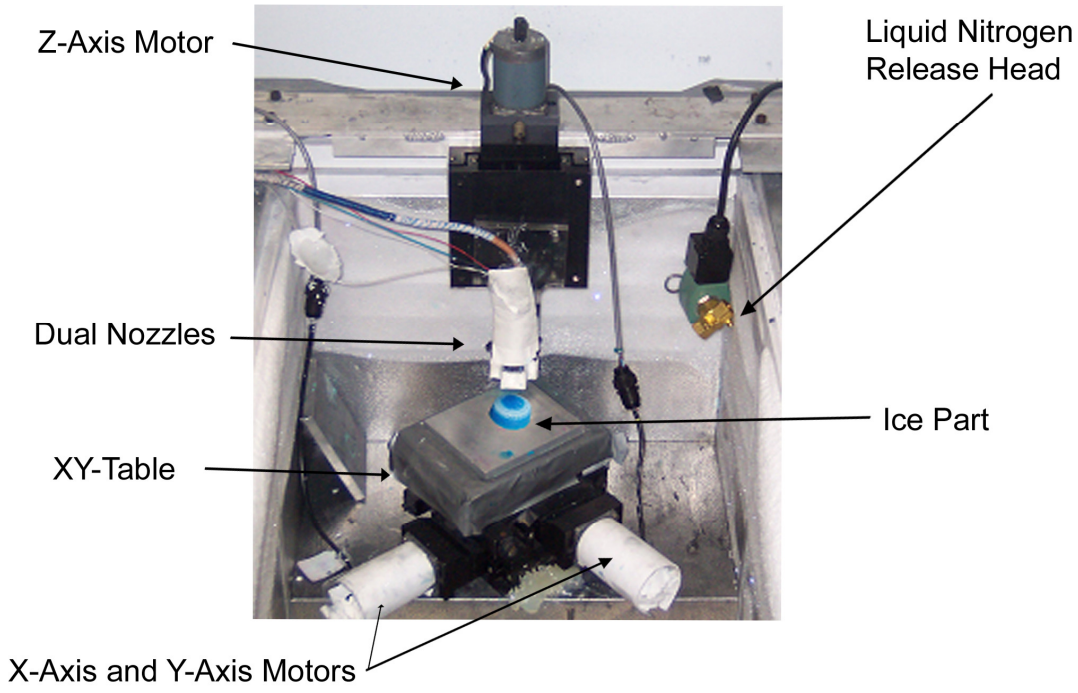

Figure 1.2. RFP build area within the freezer

A photo of various ice parts is shown in Figure 1.3. These ice parts have been made in the RFP setup without the use of support material, since their geometries are such that the walls are no more than 45° from the vertical. Dye is added to the water used and can be easily changed to build multi-colored ice parts.

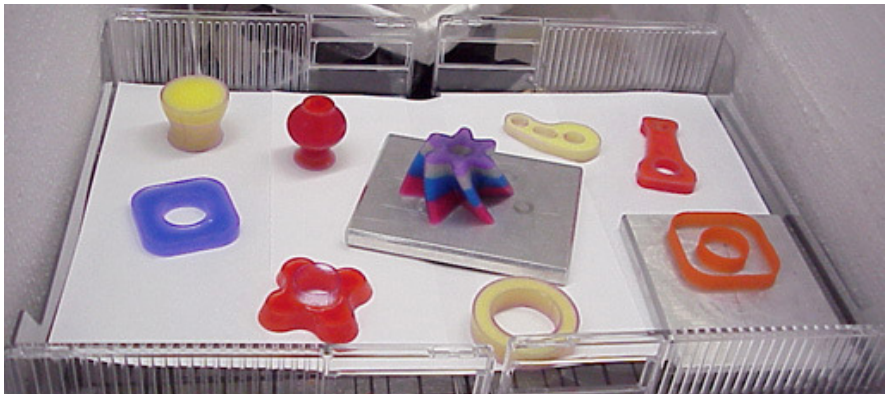

Figure 1.3. Example ice parts

Figure 1.4 shows a thin walled ice structure created from the RFP process. The inner cylinder is one continuous line while the outer gear shape is an additional continuous line for each layer.

Figure 1.4. Thin walled ice structure

The nozzle used in the RFP setup is a precision micro-dispensing drop-on-demand nozzle which is opened cyclically by a function generator. The nozzle has water, or support material, supplied to it via a Teflon tube. Once the water leaves the Teflon tube, it enters the nozzle. The internal section and components of the nozzle are made from stainless steel, polyphenylene sulfide, polyetheretherketone, ethylene/propylene rubber, butyl, epoxy, and sapphire [The Lee Company, 2008]. The materials that comprise the feed tube and nozzle that the water or support material comes into contact with before deposition are important because if the liquid significantly adheres to these materials, the flow rate will be decreased significantly due to adhesion. The materials are chosen so that the water or support material will flow through with minimal adhesion.

A local cooling system was installed in the RFP setup so that lower build ambient temperatures could be achieved and utilized. The local cooling system consists of a

liquid nitrogen supply, a solenoid valve which opens on demand and a vacuum jacketed transfer hose. The local cooling is controlled by the software that controls the nozzle opening and x-y positioning system. The liquid nitrogen can provide a temperature as low as -196 ° C when the liquid is dispensed from the tank into the surrounding region around the nozzle. The nozzle has a wire heater and a heated block that houses the complete nozzle head. The heaters keep the material in the liquid phase until it is deposited.

Many ice parts of various geometries have been successfully built with the RFP setup. Generally, vertical walls and slanted walls up to 45 ˚ off the vertical axis do not require the use of support material. Creating ice parts with the use of support material is crucial in the RFP development so that parts with overhung areas and internal voids can be built. This is necessary in order for the RFP process to be capable of producing complex parts.

A sacrificial support material, which is a eutectic sugar-water solution, has been identified for making ice parts of complex geometries and overhung areas [Bryant and Leu, 2004]. The support material used in the RFP process is miscible with the main build material, which is water that freezes to ice, so there is a great potential of diffusion between the two materials.

Understanding the interaction between the main material and the support material is a main component of this dissertation research. After understanding the interaction between the two materials thoroughly, the build parameters can be controlled such that the interaction is kept to a minimum, and dimensionally accurate, complex ice parts can be fabricated.

There have been extensive studies conducted on the RFP process without use of support material. Liu and Leu [2004] considered the solidification time in RFP, but their model only considered the main build material (water). Geometric features and surface finish of completed ice parts have also been studied [[a]Sui and Leu, 2002]. Existing literature in the area of predictive models for layer-by-layer manufacturing in which support material is concerned is extremely limited. There has been some work in the area of thermo-mechanical modeling for a freeform fabrication process that has characteristics similar to RFP. Chin, Beuth and Amon [2001] investigated the thermal and mechanical interactions between existing and new layers in Shape Deposition Manufacturing (SDM), which used stainless steel for a build material and copper for a support material. The model derived, however, only took into account the build material for the SDM process (stainless steel). Other methods were studied with respect to using multiple materials, though those processes generally were not dedicated rapid prototyping methods. Laser cladding is a process in which a powdered material is melted by use of a laser in order to coat part of a substrate. Kar and Mazumder [1988] derived an analytical one-dimensional model to study the mass and heat transfer during a laser cladding process. Their model, along with associated assumptions, solved differential equations for temperature and concentration by reducing the equations to first-order nonlinear ordinary differential equations and then solved the equations with Runge-Kutta method.

Information regarding the fabrication of complex ice parts with the use of support materials during the fabrication process, however, has not been studied previously.

1.2 PROJECT OBJECTIVES

The research presented here has the objective to provide the information needed to fabricate ice parts with supported sections by using a sacrificial support material. The work first aims to determine how the RFP process parameters contribute to the finished dimensions and surface finish of the ice part. The work then investigates a suitable support material for use in RFP.

Another objective of this research is to understand exactly what phenomenon is occurring during the build process of RFP, specifically when the main and support materials are in contact. Understanding what is occurring during the fabrication is important so that the system can be programmed to reliably build ice parts. Developing and verifying a temperature model and a concentration model is a part of this research.

There are also some other challenges within this process that this research aims to address. The temperature in the build region must be low enough to have a stable line of ice or support material, otherwise the quality of the ice part is compromised. Having a low build temperature is desirable because the wait time for the materials to freeze is lower at a lower temperature. On the other hand, having an extremely low build temperature (< -40 °C) has problems due to frost formation on the ice structures. Also, the temperature has to be high enough to allow the hardware to work properly, otherwise the dimensional accuracy of the ice part will be in jeopardy. Finding a temperature that balances these factors is investigated in this work. The temperature is also crucial in determining how cold to have the build temperature in order to prevent diffusion as much as possible, yet still be able to deposit both water and support material in a liquid state, and subsequently freeze. Furthermore, removing the support material from the

completed ice structure is of concern, due to the potential of melting the intended ice features of the finished part. Removing the support material completely is important because any residual support material alters dimensions, but a harsh removal process can also damage the ice structure.

The work also aims to qualitatively justify what build temperature is necessary to provide dimensional accuracy and prevent as much degradation to the ice as possible. The intellectual merit and broader impacts of this dissertation study are as follows:

Intellectual Merit – This research generates fundamental knowledge for the rapid freeze prototyping process. The issues addressed in this research are relevant to other droplet-based rapid prototyping processes which use a main build material and a support material. The modeling, analysis and experimentation approaches developed in this study may also be used in a groundwork to develop new types of rapid prototyping processes or to develop new materials for existing rapid prototyping schemes.

Broader Impacts – The results of this study can potentially impact areas from education to commercial uses. The models derived here could be used as a basis in research for other layered fabrication methods. Ice parts created with a higher dimensional accuracy as a result of this study have greater potential to be used as investment casting patterns.

1.3 OVERVIEW OF DISSERTATION

A brief synopsis of each section of this dissertation is given below.

Section two focuses on using water to create simple ice structures and on the process parameters in RFP. By varying process parameters, build dimensions for ice parts can be altered.

Section three is dedicated to an in-depth discussion of the support material used in RFP. The selection criteria are discussed and some ice parts built with support sections are shown.

Section four presents a thermal model that sets a foundation for the subsequent section, i.e. the concentration modeling. The thermal modeling is aimed at understanding what temperature changes are occurring during the ice part fabrication where the main and support materials are used in succession.

Section five discusses concentration modeling for RFP studies. Two types of concentration models are presented and then compared with experimentally collected data.

Section six presents information on the dimensional accuracy and surface finish of fabricated ice parts, where various build parameters have been considered. Surface roughness of ice parts was measured on the ice surfaces that were deposited as the intended ice structure and also on the ice surfaces where support material has been removed.

Section seven concludes the research work in this dissertation.

2. EFFECTS OF PROCESS PARAMETERS

A study on the effects of RFP process parameters including the nozzle scan speed, droplet size, and droplet frequency in building ice parts with a single-nozzle work head is discussed in this section. The results presented here indicate that these process parameters determine the ice layer thickness and ice line width, which in turn determine the surface roughness and the waiting time required after depositing each layer of water (i.e. between successive layers) during the ice part building process.

The freezer used in the RFP setup is a standard chest-type commercial freezer that is set to –20 °C. The nozzle opening and closing can be operated in a range of 200 to 900 Hz. With a clean nozzle allowing water to flow through without constrictions, the frequency does not change the flow rate. This is further discussed in subsection 2.3. The nozzle in enclosed in an aluminum block that has a heat source that prevents the water from freezing while it is waiting to be dispensed. The water is generally released from the nozzle at a height of 3-5 mm onto an aluminum plate, which is the substrate.

2.1 ANALYSIS OF VARYING PROCESS PARAMETERS

The current RFP setup, which was shown in Figure 1.1, has two process parameters that can be varied. By changing one or both of these parameters, the layer thickness and line width will change. The changeable parameters are the water feed rate, f, and the scan speed, v. The water feed rate is controlled by the water pressure, P, and the nozzle diameter, d. The water feed rate is calculated and measured in mm^3/s. The water pressure is varied and controlled by the height difference in the water source and nozzle. The scan speed is encoded into the program that controls the X-Y table. The scan speed is measured in mm/s.

To begin the study of the water feed rate, the droplets that are released from the nozzle are considered. The droplet size is dependent upon the diameter of the nozzle and the surface tension of the water. The following equation can be used to determine the amount of mass contained in a single droplet [Brodkey, 1967]:

$$m = \frac{\pi d \sigma F(d/V^{1/3})}{g} \tag{1}$$

where m is the mass of the droplet, d is the nozzle diameter, σ is the surface tension of water, V is the volume of the droplet, g is the gravitational constant, and $F(d/V^{1/3})$ is an empirical correlation function. It is assumed that in this case the empirical correlation function has a value of 1, which means that there are no satellite drops formed and there is not any water left hanging at the tip of the nozzle. Equation 1 can be used to determine the number of droplets being released by the nozzle in each opening pulse. This is a concern for higher frequency settings, since the nozzle could be open for such a short amount of time that not enough water could flow through to create a single drop, thus the water feed rate would be inconsistent and hard to predict.

The water feed rate can be found by considering an inviscid flow, which is acceptable for this flow [Fay, 1994]. Bernoulli's equation is used to determine the velocity of the water flowing as if the nozzle were kept open continuously. The water feed rate can be calculated from the diameter of the nozzle, the duty cycle set for the nozzle through the function generator (which is the percentage of time the nozzle is actually open), and the height difference between the nozzle and the water containment unit as follows:

$$f = \frac{\pi}{4} d^2 N \sqrt{2g\Delta h} \quad (2)$$

where d is the nozzle diameter, N is the duty cycle of the function generator, g is the gravitational constant and Δh is the height difference between the nozzle and the water supply unit. The nozzle must be clear and free of contaminants to produce good results with a low error between the calculated and measured mass of water.

As soon as the water droplets come into contact with the substrate, the droplets combine and form a continuous water line before freezing. The length of this line is calculated by multiplying the scan speed, *v*, by the time, *t*, taken to create the section. The volume of this line is Avt, where A is the cross sectional area of the line. The volume of the line is also equal to the water feed rate, *f*, multiplied by time *t*. Setting these two equations equal to each other gives the cross-sectional area of a water line:

$$A = f \ / \nu \quad (3)$$

Figure 2.1 shows a typical section of the ice wall after some layers have been deposited. From this figure, a relationship between the layer thickness and line width can be found. This relationship is:

$$\Delta z = w \cdot \sin(\alpha/2) \quad (4)$$

By combining equations (3), (4), and the relationship $A = w \cdot \Delta z$, the layer thickness and line width can be derived as:

$$\Delta z = \sqrt{\frac{f \cdot \sin(\alpha/2)}{\nu}} \quad (5)$$

$$w = \sqrt{\frac{f}{\nu \cdot \sin(\alpha/2)}} \quad (6)$$

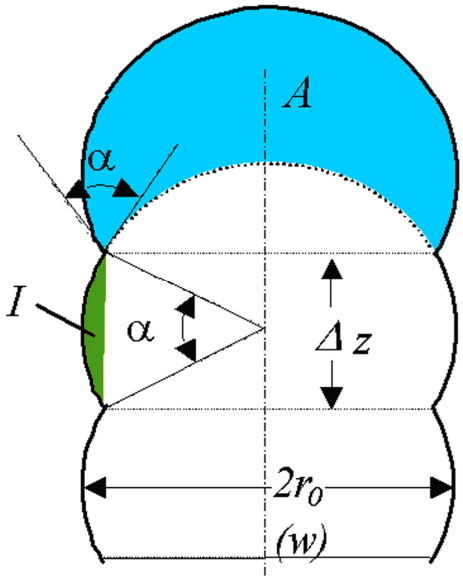

Figure 2.1. Cross-section illustration of an ice line

where α is the water-ice contact angle (see Figure 2.1), which has been determined to be 20° for water used in a -20 °C freezer [[b]Sui, 2002]. The water-ice contact angle α was determined first by measuring the layer thickness and line width in various ice parts. Equations (5) and (6) were then used to calculate α. It is seen in equations (5) and (6) that the layer thickness and line width depend on the water feed rate and the nozzle traverse speed.

2.2 SURFACE ROUGHNESS AND BUILD TIME

The layer thickness is important in any layered fabrication process because of the impact it has on surface roughness. In layered fabrication a "stair-stepping" effect could become a problem because it increases the surface roughness of the part. In RFP, layer thickness can be reduced by reducing the water feed rate or increasing the scan speed, but the total build time is then increased. The build time will be discussed later in this section. The surface roughness of ice parts built by RFP can be predicted as follows:

The definition of surface roughness, R, is:

$$R = I / \Delta z = (0.5\alpha r_o^2 - 0.5\, r_o^2 \sin\alpha)/\Delta z \quad (7)$$

where I, Δz, α and r_o are defined in Figure 2.1. α is measured in radians for surface roughness calculations. Using Figure 2.1 and equation (5), it can be seen that

$$r_o = \frac{w}{2} = \sqrt{\frac{0.5f}{v\sin(\alpha/2)}} \quad (8)$$

So, by substituting equations (5) and (8) into (7), the surface roughness is obtained as:

$$R = k\sqrt{f/v} \quad (9)$$

where

$$k = \frac{(\alpha - \sin\alpha)}{8\sin^{3/2}(\alpha/2)} \quad (10)$$

Equation (9) shows that the surface finish is dependent upon the variable process parameters of RFP.

The build time for an ice part strongly depends on the minimum wait time between successive layers. The minimum wait time is the time required for freezing after a layer has been deposited and before depositing the next layer to ensure the previous layer is solidified and residual heat has been dissipated. By using a moving heat source, [Sui and Leu, 2003] showed that the minimum waiting time between two successive layers is:

$$t_{\min} = \frac{E \cdot \Delta z}{\lambda \cdot \Delta T\sqrt{b}}\sqrt{1 + \frac{\lambda \Delta T}{E\phi}} \quad (11)$$

where E is the enthalpy, Δz is the layer thickness, λ is the thermal conductivity, ΔT is the difference between the water and the freezing temperature, $b=2h/\lambda w$, h is the heat transfer

coefficient, w is the layer width, and ϕ is the thermal diffusivity. For normally used values of Δ T in RFP, $\lambda \cdot \Delta T$ is far less than $E\phi$. Equation (11) thus can becomes:

$$t_{\min} = \frac{E\Delta z}{\lambda \cdot \Delta T\sqrt{b}} \tag{12}$$

By substituting (5) and (6) into (12), Equation 13 is obtained:

$$t_{\min} = \frac{E \cdot \sin^{1/4}(\alpha/2)}{\Delta T\sqrt{2h\lambda}}\left(\frac{f}{v}\right)^{3/4} \tag{13}$$

The enthalpy can be calculated as E = ρ (L + cΔ T), where ρ is the water density, L is the latent heat of fusion, and c is the specific heat. Equation 13 shows that the minimum wait time between layers and thus the part build time can be changed by varying the process parameters which affect the layer thickness and line width.

2.3. EXPERIMENTAL RESULTS

The water feed rate was measured and compared to the predicted value obtained from equation (2). The diameter of the nozzle, d, is 0.003 in (0.0762 mm), the duty cycle is set to 50%, and the height difference, Δh, is 3158 mm. Using these values, the water feed rate is predicted to be 17.95 mm^3/s. The measured water feed rate, taken from an average using 5 different nozzle frequencies, is 18.76 mm^3/s. There is an error of 4.3%. In order to achieve a good comparison between the predicted water feed rate and the measured water feed rate, a clean, unclogged nozzle must be used. It has been observed that as the nozzle starts to get clogged, the mass flow rate increases as the nozzle frequency increases. This is due to a long throw bladder contained in the nozzle that will force more water out through the constriction when there are more openings per second

due to the higher frequency [The Lee Company, 2008]. So using a clean, unclogged nozzle is important in order to produce accurate ice parts.

Equation (1) was used to determine if the nozzle was opened for a long enough period for each pulse to produce at least one droplet. The height difference was again set at 3158 mm, but the duty cycle of the function generator was decreased to 20% (which is the lowest feasible duty cycle for the equipment used in the research). The diameter of the nozzle was the same as before, which is 0.0762 mm, the surface tension of water is 7.34E-2 N/m, and a value of 1 was used for the empirical correlation function. The number of droplets produced at this water pressure was at least one droplet per pulse in the nozzle frequency range of 200 to 900 Hz. Figure 2.2 shows the predicted number of droplets per nozzle pulse.

Ice walls and cylinders were fabricated with varying water feed rates and the layer thickness was measured. The scan speed was set to 50 mm/s. The layer thickness agreed well with the calculated values using equation (5), with the error ranging from 1.8% to 16.3%. Figure 2.3 shows the comparison between the predicted layer thickness and the measured layer thickness at various water feed rates.

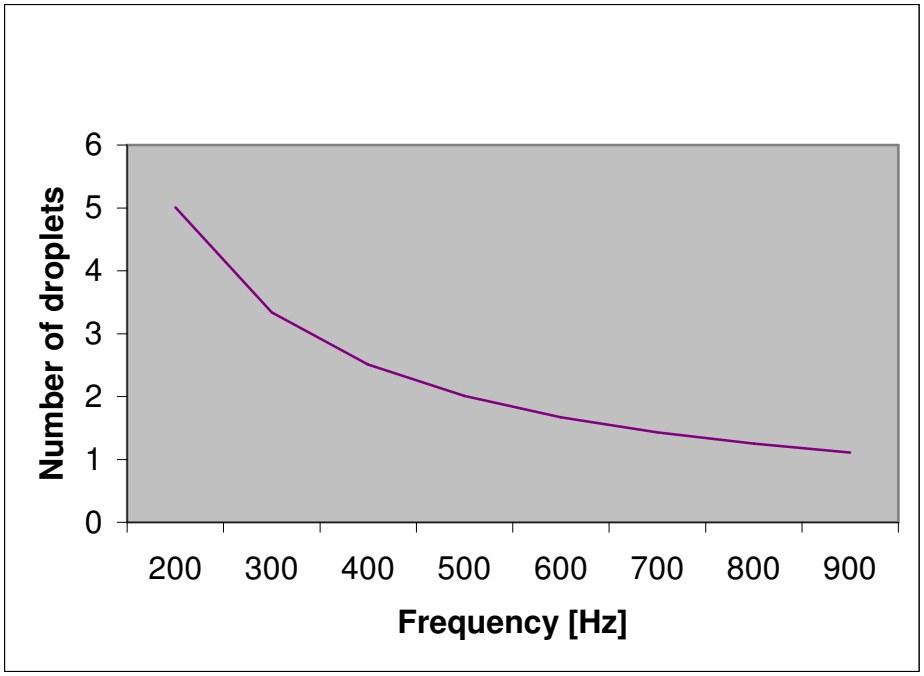

Figure 2.2. Predicted number of droplets released at 20% duty cycle

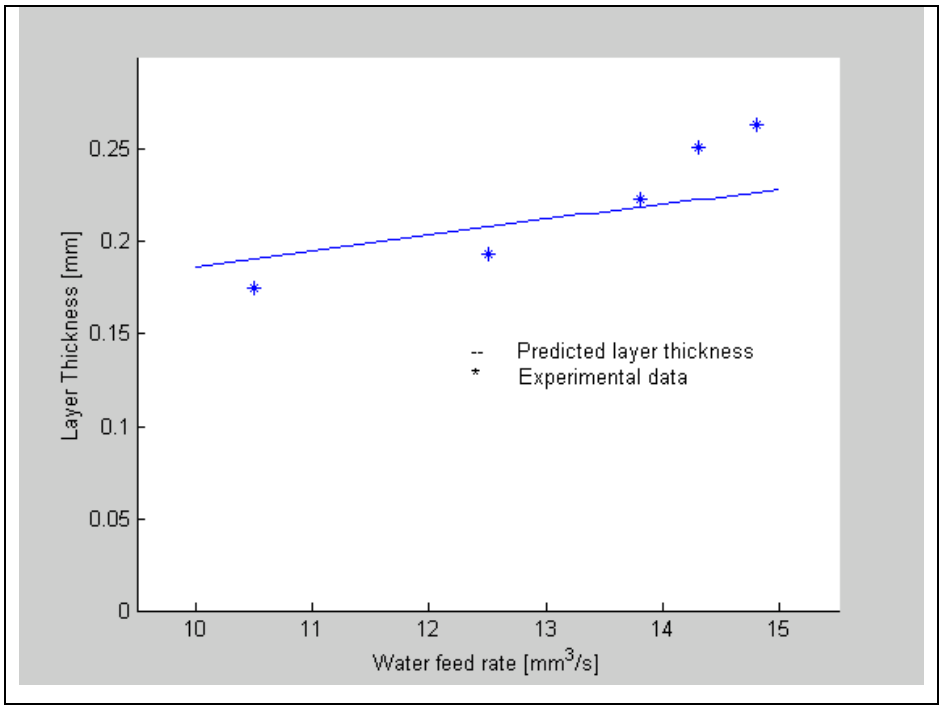

Figure 2.3. Comparison of predicted and measured layer thickness

2.4. CONCLUDING REMARKS

The variable process parameters in RFP, which are the water feed rate and the scan speed, can be varied to achieve the desired layer thickness or line width. The surface roughness and minimum wait time (thus the part build time) for ice parts can be calculated with these parameters as well. The process parameters are important to consider when fabricating ice parts, since they contribute to many characteristics of ice parts. The water feed rate is controlled by the water pressure and nozzle diameter. The scan speed is encoded into the software used to operate the XY-table. Besides considering the variable process parameters, it is also important to use a clean, unclogged nozzle in the RFP process.

3. SUPPORT MATERIAL

Use of support material in RFP is necessary for building complex ice parts with features such as internal holes or overhung areas. The support material should have certain desirable properties in order for it to be incorporated into the existing RFP setup with minimal changes to the system. Being able to incorporate a support material ensures that ice parts of complex geometry can be produced by the RFP process.

3.1 IDENTIFICATION OF SUPPORT MATERIAL

The search for a suitable support material to be used in RFP proved to be a challenging and lengthy process. The support material preferably would have all of these qualities: not soluble in water, a similar contact angle to water, non-toxic and environmentally benign, easily obtainable, and easily removable from the ice by a method that will not affect the remaining structure. There were many substances considered, including a number of different types of oil. Due to oil and water being incompatible in a mixing sense, oil seemed to be a good choice. However, experiments conducted with oil found it to not work as a support material due to the inability to sufficiently solidify during freezing. After many considerations and testing of many materials, it was concluded that a support material fitting all of the prescribed criteria would probably not be identified in a timely manner. However, by removing one criterion, the condition of not soluble in water, a couple of materials that could be used as a support material were identified. A possible solution at the top of the list for a support material was a eutectic salt (NaCl) solution, and the second choice was a eutectic sugar (dextrose) solution. Figure 3.1 shows the phase diagram for the salt solution, while Figure 3.2 shows the phase diagram for the sugar solution. Table 3.1 lists the

concentration values at the eutectic point and melting point of each solution [Jackson and Silsbee, 1922].

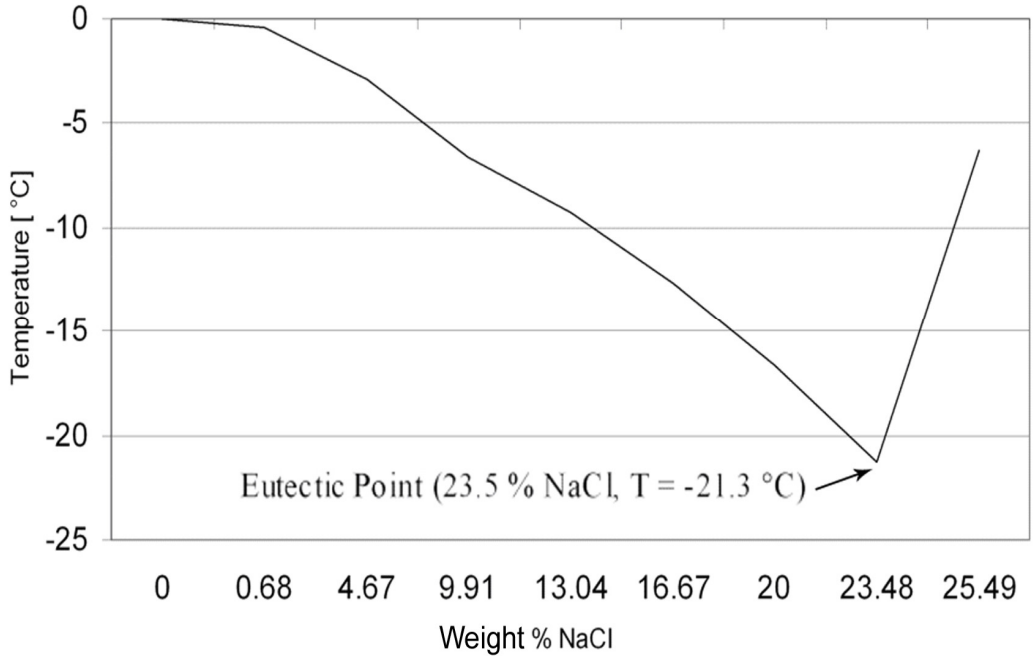

Figure 3.1. Phase diagram for a salt/water solution

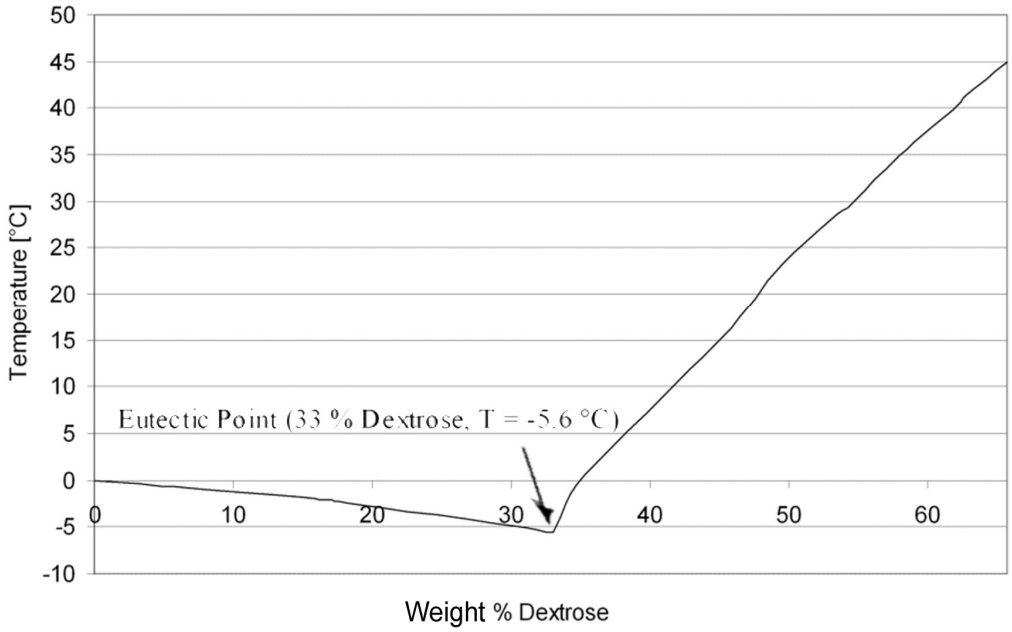

Figure 3.2. Phase diagram for a sugar/water solution

Table 3.1. Properties of support material considerations

Solution	Concentration (by weight)	Melting Point
$NaCl - H_20$	23.5 % NaCl	-21.3 ˚ C
$C_6H_{12}O_6 - H_2O$	33 % $C_6H_{12}O_6$	-5.6 ˚ C

The salt solution was initially considered to be the first choice due to the large temperature range in which the support material could be melted. This selection would provide more than 20 degrees difference in the melting points between water and the support material. The building of the ice part would need to be done in a freezer colder than the melting point of the support material, then placed in a freezer that is set slightly above the melting point of the support material. From the control aspect, the larger temperature difference was preferred.

In order to check the interaction of the two candidate solutions with ice during the removal process, some qualitative experiments were first done. A known amount of water was frozen completely, then a known amount of the support material consideration was put on top of the ice and allowed to freeze. This was done in a –60 ˚ C freezer to ensure that both materials were completely frozen. In the experiments conducted with the salt water solution, the ice and frozen salt water ice part were brought up in temperature to -20 °C to remove the salt water portion. In the case of the sugar water solution, the ice parts were brought up in temperature to -5 °C. In both cases, a room freezer was used in the removal of support material. The details and results of these experiments are given in Table 3.2.

Table 3.2. Amount of ice loss when support material is removed at -20 °C for the salt solution and -5 °C for the sugar solution

Solution	Trial no.	Initial H_2O weight (g)	Initial support mat. weight (g)	Final ice weight (g)	% difference of final ice weight to initial H_2O weight
Sugar	1	12.08	10.25	12.04	-0.33
Sugar	2	9.97	10.25	9.81	-1.60
Sugar	3	11.34	10.89	11.18	-1.41
Sugar	4	9.66	10.77	9.50	-1.66
Sugar	5	10.13	10.36	9.89	-2.37
Sugar	6	10.66	10.98	10.43	-2.16
Sugar	7	15.33	11.37	14.94	-2.54
Sugar	8	13.02	10.64	12.88	-1.07
Salt	1	9.71	11.41	6.36	-34.50
Salt	2	10.03	11.57	6.60	-34.20
Salt	3	9.81	10.13	6.26	-36.20
Salt	4	9.74	11.56	5.81	-40.30
Salt	5	9.67	11.24	7.01	-27.50
Salt	6	9.76	11.18	7.29	-25.30
Salt	7	9.81	11.33	7.46	-24.00
Salt	8	9.72	11.20	7.35	-24.40

The last column in Table 3.2 indicates the impact of the support material on ice. The salt solution is this experiment degraded the ice up to 40.3 % by weight. However, Table 3.2 shows that the interaction between the sugar solution and the ice is much lower, where the difference in the amount of ice from that at the end of the experiment to the initial amount of water was less than 3% each time. Upon further inspection of salt and sugar properties, it was found that the NaCl molecule is significantly smaller in size than

the dextrose molecule and it is likely that the NaCl molecules disrupt the ice crystalline structure much more than the sugar molecules, which is consistent with these experimental results. Thus, the sugar solution was considered the choice for support material to be used in RFP. Table 3.3 summarizes the properties of water/ice and the sugar solution, which are used in the analysis in this research.

Table 3.3. Properties of water/ice and the sugar solution support material

	H_2O	$C_6H_{12}O_6(33\%) - H_2O$
Density p_{solid} p_{liquid}	 917 kg/m^3 1000 kg/m^3	 917 kg/m^3 1140 kg/m^3
Specific Heat Cs (solid) Cl (liquid)	 2094 J/kg-°C 4174 J/kg-°C	 1404 J/kg-°C 2800 J/kg-°C
Thermal conductivity(λ)	0.6 W/m-°C	≈ 0.6 W/m-°C
Latent heat of fusion(L)	335000 J/kg	234000 J/kg
Heat transfer coefficient (h)	8.66 W/m^2-°C	≈8.66 W/m^2-°C

The properties listed in Table 3.3 for the eutectic sugar solution were calculated using various methods. The liquid density was measured directly. The density of the solid state for the sugar solution was estimated using the corresponding percentages of each material combined. The specific heat was estimated by taking the value of the specific heat of sugar as it comes out of a saturated solution and combining it with the corresponding amount of water that comprises the solution. The thermal conductivity and heat transfer coefficient were assumed to be very close to the values for water, since the addition of sugar most likely will not change these properties significantly. The latent

heat was calculated by assuming the two constituents of the solution contribute in the same ratio as the mass of each that constitutes the solution. These material properties are not readily available in publication for the eutectic sugar solution, thus approximation was necessary for this study.

Since the support material has a higher viscosity than water, using the support material in the drop-on-demand nozzles was of concern. In order to verify that the support material could be used in the RFP setup, a cylinder part with a middle section consisting of support material was built. Figure 3.3 shows one of the cylinders that was built, where the ice sections are blue (due to an added dye), and the support material section is white (no dye is added to the support material). Figure 3.4 shows the part after the support material has been removed via a temperature difference. The part was placed in a -5 ° C freezer overnight to remove the support material. It can be seen in Figure 3.4 that there is considerable diffusion occurring between the ice and the support material, as seen by an uneven edge, when the support material is being built upon by the water/ice.

Figure 3.3. Ice part before support material is removed

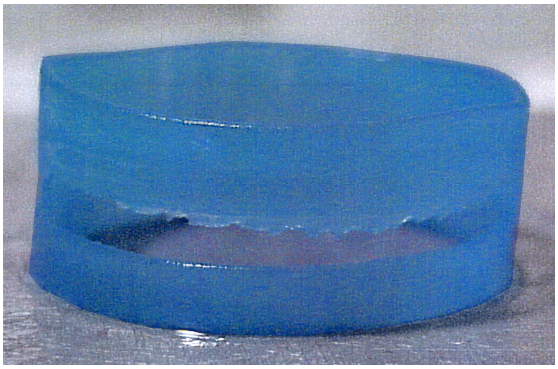

Figure 3.4. Ice part after support material is removed

Figure 3.5 shows a close-up, color enhanced photo of the uneven interface section from Figure 3.4. Each part of the photo is described with text in the photo. This uneven edge produced is a result of diffusion of the sugar from the support material section of the wall into the water section, which in turn alters the melting temperature of that region.

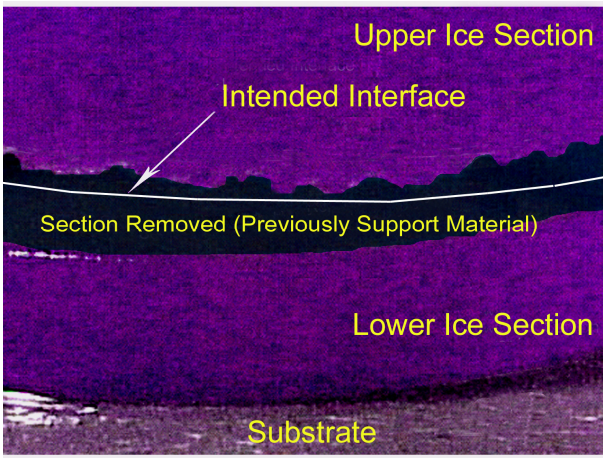

Figure 3.5. Close-up view of boundary between support and main build material

The boundary where ice is the lower material and the support material is deposited on top does not have this uneven boundary. This smooth edge can be seen in

Figures 3.4 and 3.5. This is due to water having a higher specific heat than the support material, which was shown in Table 3.3. Consequently, when the support material is the lower surface and water is being deposited on top, the not-yet-frozen water melts the support material, the two solutions mix and the mixture that freezes has a concentration somewhere between the eutectic point of the sugar solution and pure water, so the melting point is consequently altered as well. When support material is deposited onto already frozen water/ice, there is a much less risk of the already frozen water/ice being melted because latent heat can easily be absorbed by ice without significantly melting.

3.2 DIFFUSION BETWEEN SUPPORT MATERIAL AND MAIN MATERIAL

In order to minimize the above described melting, mixing, freezing/re-freezing process, which produces an uneven boundary edge, the water needs to freeze very quickly on top of the frozen support material so as to shorten the diffusion time as much as possible. Diffusion occurs substantially only during the liquid phase, so shortening the time that the material is in the liquid phase as much as possible is required. Typically, liquid-to-liquid diffusion has a diffusivity value of 10^{-9} to 10^{-6} m^2/sec, whereas solid-to-solid diffusion typically has a diffusivity value of $5x10^{-14}$ to $1x10^{-10}$ m^2/sec [Crank, 1956]. Because the large difference between liquid and solid diffusion, liquid-to-liquid diffusion is considered the primary cause and the liquid-to-solid and solid-to-solid diffusion is considered negligible in this study.

The approach taken to quickly cool the deposited water line was to use a local cooling system. This produced a cooler local region around the deposition, which then decreased the freezing time of the water and/or the support material. The reasoning behind this can be seen by considering the 1-D conduction heat transfer equation:

$$\frac{1}{\phi}\frac{\partial T}{\partial t} = \frac{\partial^2 T}{\partial x^2} + m(c\Delta T + L) \qquad (14)$$

where ϕ is the thermal diffusivity, T is the temperature, t is time, m is the mass, c is the specific heat, ΔT is the temperature difference, and L is the latent heat of fusion.

By using Equation 11 to solve for the minimum wait time between layers, the time which will allow heat to be dissipated sufficiently such that each layer can freeze without residual heat build-up can be found for both main and support materials. The properties of water and the support material can be found in Table 3.3. If the layer height and width are assumed to be the same for water and the support material and are set to the typical dimensions of 0.17 mm and 1 mm, respectively, Equation 11 can be used to find the minimum wait time between each layer for both water and the support material. By allowing this amount of wait time between every two adjacent layers, each layer will have had a sufficient amount of time to completely solidify.

Figure 3.6 shows that as the ambient temperature around the deposited line is lowered, the freezing time is decreased, as predicted by Equation 11. When the freezing time is decreased, the time that diffusion can occur is also decreased. ΔT is the key to the idea of local cooling. By maximizing ΔT as much as possible, the acceptable minimum wait time is reduced. Based on Figure 3.6, the wait time decreases to under 2.5 seconds for both water and support material if the temperature around the newly deposited line reaches -195 ° C.

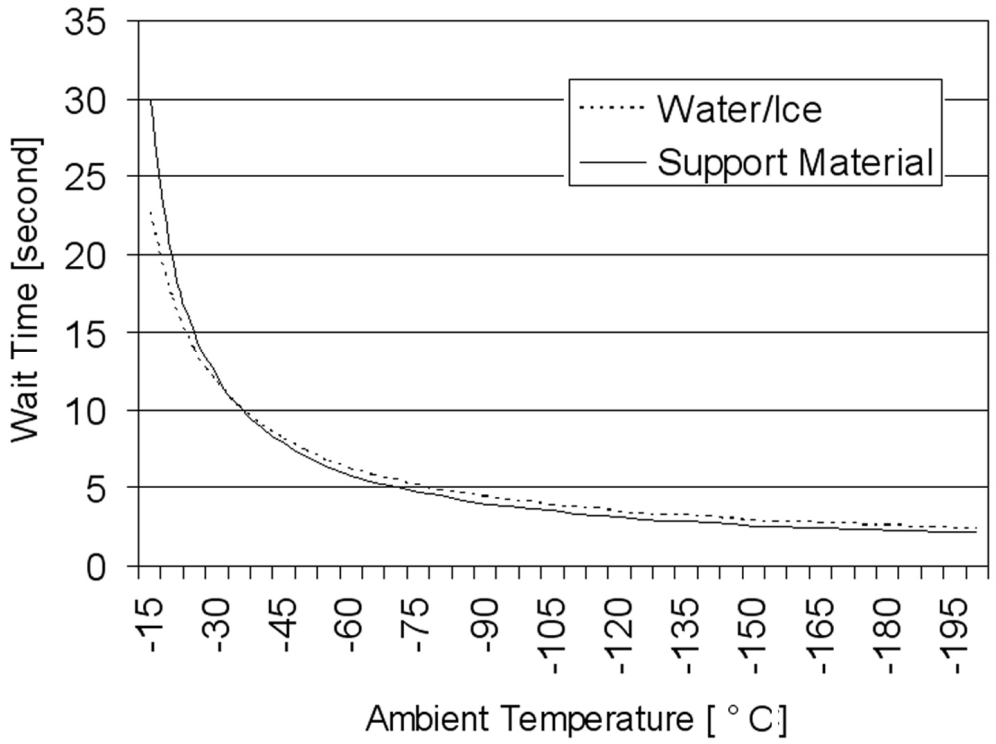

Figure 3.6. Minimum wait time between layer deposition

In order to achieve very low ambient temperatures, a liquid nitrogen source was installed in the RFP setup to achieve local cooling. Liquid nitrogen at atmospheric pressure is -196 ° C. By using the liquid nitrogen as a source of extra cooling, the local ambient air around the line deposition can be substantially cooled. This allows much faster freezing, thus eliminating or drastically reducing diffusion between the underneath layer and the newly deposited layer. Figure 3.7 shows a cylindrical ice part that was built with additional local cooling using the liquid nitrogen source. It can be seen in this figure that the interface surface between the support material layer and the ice layer above it is now visibly smooth and there is no apparent indication of diffusion.

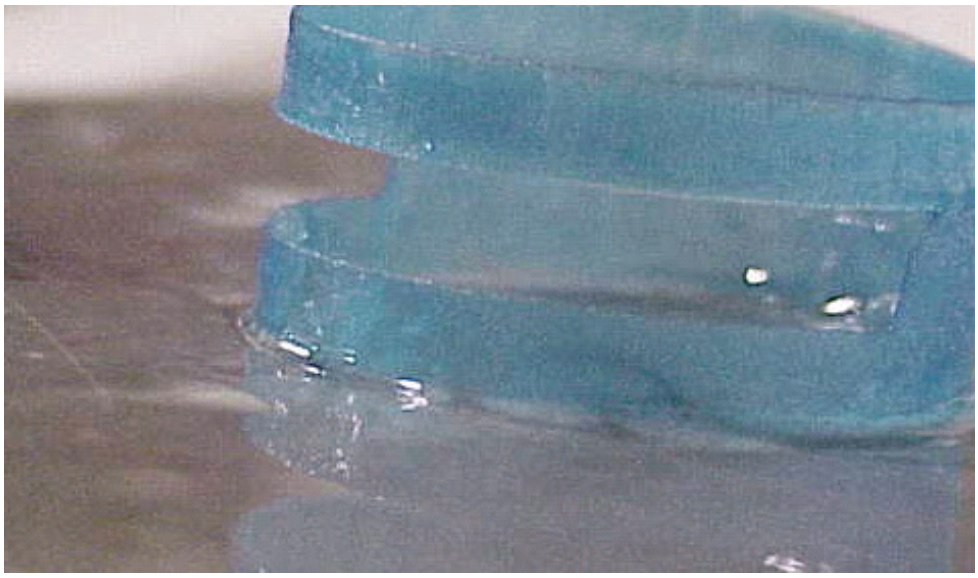

Figure 3.7. Ice part with no indication of diffusion

3.3 BASIC CONCENTRATION MODEL

In order to understand the diffusion phenomenon and predict the amount of diffusion that is occurring around the interface of the two miscible materials, a basic concentration model is developed. The model takes into account a thin wall of support material and ice. The support material is the lower material, or the first deposited. The water, freezing to ice, is the second material deposited since this would represent the most challenging diffusion scenario. The concentration model is aimed to predict the concentration changes near the interface of the two materials and determine how much degradation to the ice structure will occur after removing the support material.

The direction of diffusion of the sugar molecules is from the support material to the water layers (i.e. from higher sugar concentration to lower sugar concentration). These heights are denoted as ‘a’ and ‘b’ in Figure 3.8. The line between ‘a’ and ‘b’ represents where the actual deposited interface would occur. The height ‘a’ represents the height of the deposited water/ice wall that is affected by diffusion of sugar and will be

removed during the later support material removal. Height ‘b’ represents the depth in the support material wall that is affected significantly, although this height is not as important to predict since it is in the area that is intended to be removed after complete fabrication of the wall.

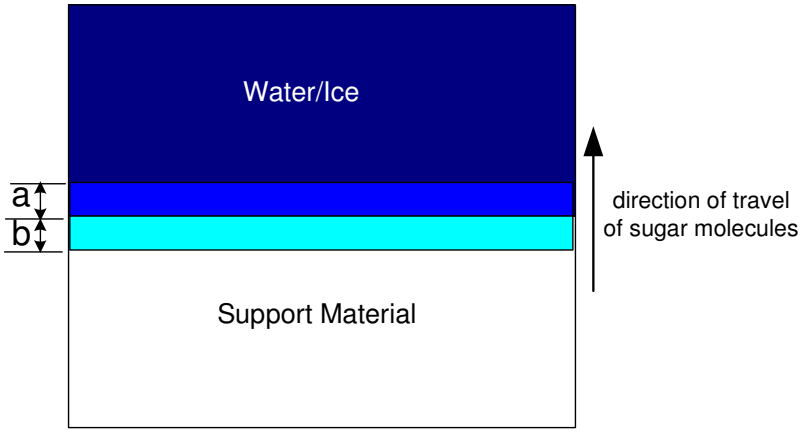

Figure 3.8. Diffusion considered in a thin wall

The support material used in the RFP process has a melting temperature of -5.6 °C, whereas water has a melting temperature of 0 °C . When the water and support material mix during fabrication, however, the melting temperature of the affected region (i.e. ‘a’ and ‘b’ in Figure 3.8) is altered, due to the change in the composition where mixing occurred. Water has a higher latent heat than the support material, so when water is deposited onto already-frozen support material, there is a possibility for the support material to melt. The reverse scenario does not pose a problem, because the liquid support material does not significantly melt the already-frozen ice layers due to its lower latent heat. When melting occurs, the water and support material will mix, and then re-freeze due to the low ambient temperature. The mixing of the two materials during the liquid phase is the most important time to consider, since the diffusivity between two liquids is much higher than for a solid in contact with a liquid or a solid-to-solid contact.

A one-dimensional concentration model based on Fick's first law was developed to give some initial predictions and trends as to how many layers were affected by diffusion when water was deposited onto a layer of already frozen support material [Bryant and Leu, 2004]. The model takes into account the latent heat released by the volume of water in a layer. The water freezing will melt the layers of support material below, mix and then the layers will freeze again, but have different concentrations. Fick's law states that the mass flux of a solute, J, into an area of less concentration can be calculated by a diffusion coefficient, D, multiplied by the differential of the concentration over the distance traveled. Computation of the flux of sugar molecules that will go from the area of higher concentration (i.e. the support material) into the lower concentration areas (the water layer) is based on the following equation.

$$J = -D\frac{\Delta C}{\Delta x} \tag{15}$$

where J is the flux of sugar that migrates from the area of higher concentration to lower concentration, D is the diffusion coefficient, C is the concentration and x is the distance that the sugar molecules travel (i.e. the layer height).

The assumptions taken into account in this model are:

1. The diffusion constant, D, is a general value for liquid materials, but a low value is used due to the liquid freezing. This assumption is taken due to not having a value available specifically for mixing of water and a water/sugar mixture.
2. Each layer is assumed to completely mix, so the layer will be modeled to have the same concentration throughout the entire layer.
3. One-dimensional diffusion only is considered.

The model used the minimum wait time from Equation 11 as the amount of time during which diffusion occurs. The ambient temperature is an input and it will change the amount of diffusion predicted by the model. Some results from the model for different ambient temperatures are shown in Figure 3.9. The layers of support material are noted in the figure and the layers of water that have been deposited on the frozen support material have the predicted concentration for each layer noted in the figure.

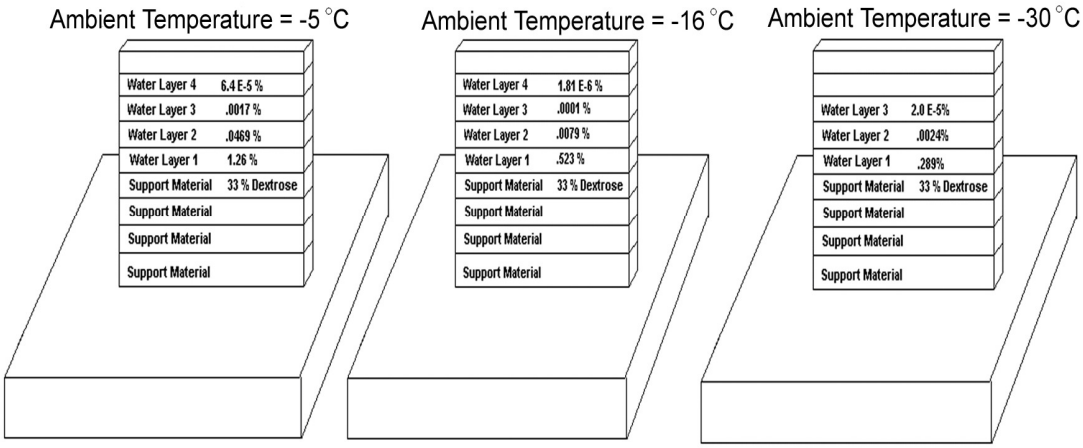

Figure 3.9. Example of layer concentration predictions by using Fick's First Law

The above model was developed as a rough initial estimate in order to predict a trend for concentration changes occurring in a wall built with water and support material. The concentration model is difficult to verify experimentally, since the concentration can not be measured at any given point during the fabrication process or in a frozen structure. Using the predicted concentration results of this program and knowing the melting temperatures of water and support material, height was calculated for thin walls which would have the support material region removed in a -5 °C freezer.

3.4 EXPERIMENTAL RESULTS

In order to build with water and support material together, the height of the deposited lines must be calculated beforehand in order to allow the correct number of layers to be deposited to create the correct height. Since local cooling has been implemented into the RFP system, the contact angles of both the water and the support material were measured so that the layer height could be found. In order to check the contact angle, lines of water and support material were deposited while using local cooling and measured upon completion. By knowing the measured height and width of the walls, Equations 5 and 6 were used to find the contact angle. It turns out that local cooling affects the contact angle of water, which was 20° in a –20° C freezer. The contact angle for water comes out to be about 12° when the ambient temperature around the area being built is locally cooled (i.e. -196 °C) ambient in the local vicinity of deposition). The support material has a contact angle of about 14° when using the local cooling, so the scan speed and/or volumetric feed rate need to be changed accordingly so that the two materials may be built and have the same line height. For example, if the scan speed is set to 50 mm/s and the volumetric feed rate is 17.85 mm^3/s, the line width and the line height for ice can be found by Equations 5 and 6 to be 0.194 mm and 1.85 mm, respectively, and for the support material the line width and the line height can also be found with Equations 5 and 6 to be 0.209 mm and 1.71 mm, respectively. Since the line heights need to be the same for each material used, the support material line height is set equal to that of ice, which is 0.194 mm, and then the scan speed is recalculated using Equation 5 for the support material. The recalculated scan speed is 58.12 mm/s, vs. the

scan speed of 50 mm/s for depositing water. Using two scan speeds in the construction of an ice part enables resulting in uniform heights with the two different materials used.

Qualitative experiments were conducted to compare the predicted values obtained with this basic concentration model. Ice walls were built with a nominal height of 3.94 mm onto an already frozen wall of support material of the same height. Both materials had wall lengths of 10 mm. The predicted heights were based on the model in Equation 15 and how many layers of water would be affected by diffusion. The ice walls were placed in a -5 °C freezer for five minutes to remove the lower support material and then the wall heights were measured with Vernier calipers. If diffusion occurs, the wall height will be less than the nominal height of 3.94 mm. The ambient build temperatures for the ice walls, along with the nominal height, predicted wall height based on the concentration model, and the (average) measured wall height is shown in Table 3.4.

Table 3.4. Diffusion quantitative experiments

Ambient Temperature, °C	Nominal wall height, mm	Predicted wall height with diffusion, mm	Measured wall height, mm
-10	3.94	3.78	3.32
-12	3.94	3.78	3.56
-15	3.94	3.94	3.68
-18	3.94	3.94	3.73
-20	3.94	3.94	3.84
-22	3.94	3.94	3.89
-25	3.94	3.94	3.86
-30	3.94	3.94	3.88

Figure 3.10 shows the results of the height prediction and measurement data from Table 3.4, along with the deviations in measurements taken during the experiments and the original designed wall height.

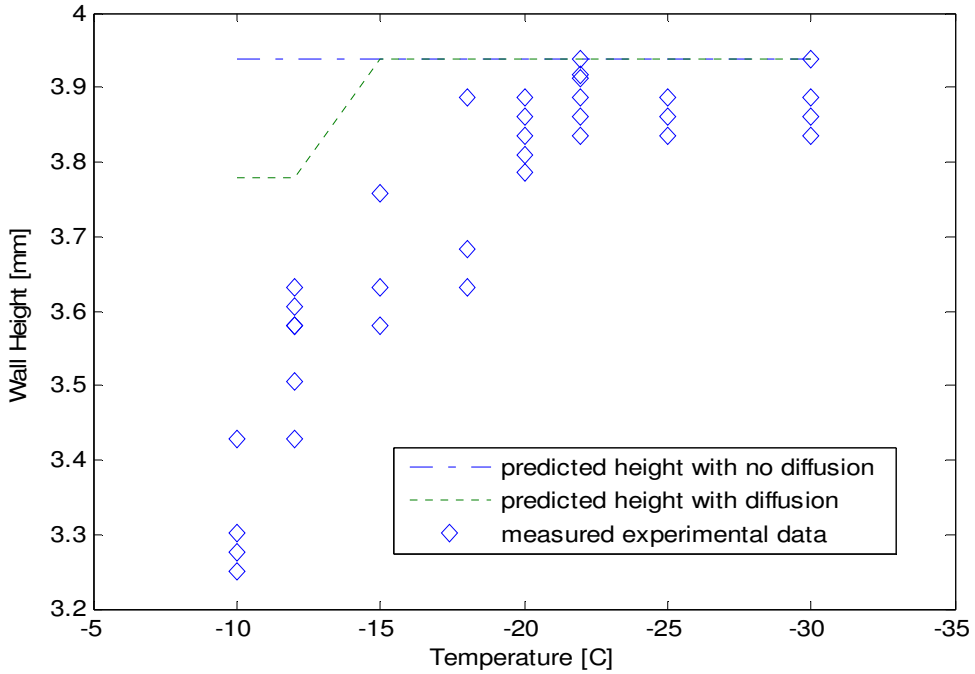

Figure 3.10: Measured height data for ice walls built in various ambient temperatures

The above simple concentration model predicted a trend which is more important to note than the actual measured values. This simplified model is the basis for a more complex model to be described in Section 5, which is necessary to fully understand the diffusion phenomenon occurring between the two materials during ice part fabrication in RFP.

The support material is not a pure substance. Rather, it is organic in nature due to the addition of dextrose. So the melting/freezing point is not an absolute defining line between liquid phase and solid phase. The support material is often in a 'mushy' state, depending of the ambient temperature. The support material removal process influences whether the 'mushy' zone will be removed or not. Initially, to remove the support material, a fabricated ice part was placed in an open ambient in a -5 °C freezer and left

overnight to allow the supported regions to melt. This removal process left the interface of the main and support material very uneven, as was shown in Figure 3.4.

In order to remove the supported regions so that the interface is a smooth surface, the support material removal process evolved to placing the ice part in the -5 °C freezer in a kerosene bath and agitating the part until the support regions were removed. The question arose as to how much dextrose must be present in the regions in order to remove that region during the support material removal process. To find out at what concentration value a region is removed in the support material removal process, experiments were conducted. Lines of support material of varying width and dextrose concentration values, representing different thicknesses of lines used in ice part fabrication, were deposited onto a substrate and allowed to sufficiently cool in a -25 °C ambient, so the lines were completely frozen. The substrates were then transferred to a -5 °C freezer and the lines were put through the same process of support material removal as an ice part would be subjected to. It was noted if the lines were removed in the process or if they remained intact. If the line was partially removed, the data was disregarded. The results of the corresponding concentration values and thicknesses in which the lines were removed in the experiments are summarized in Figure 3.11.

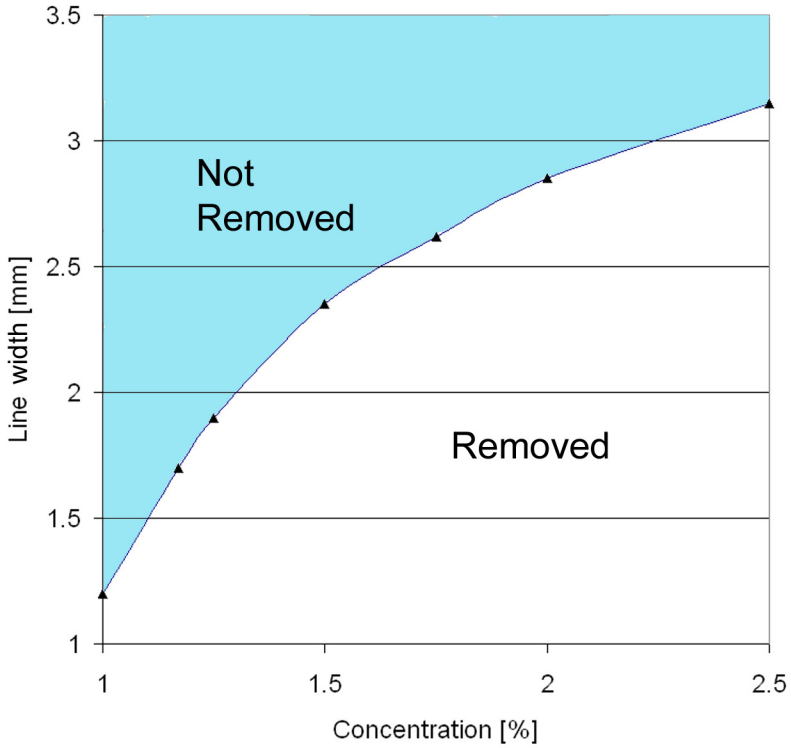

Figure 3.11. Concentration values for removal of support material at different line widths

Figure 3.11 shows that as the width increases in a line, the percent of dextrose present for it to be removed also increases. Thus, thinner lines, and thus thinner ice structures, should be removed with less dextrose present during support material removal. Depending on the thickness of ice parts being fabricated, Figure 3.11 can be referred to when determining what concentration the supported regions will be removed. Typically, thin ice structures fabricated have a thickness of approximately 1-2 mm.

This support material removal concentration guideline is useful when implementing the concentration model in Section 5.

By using local cooling and the support material, more complex ice parts have been made as shown in Figure 3.12. These ice parts were built using various techniques of process planning. Part A was built in a concentric circle fashion, starting from the

outer diameter circle and working inward to create a solid cylinder. The support material was deposited in a similar fashion around the lower cylinder to a diameter large enough to support the upper section of the ice part. Part B was built in a similar fashion, but the 'legs' were each built separately and deposited in concentric circles with support material deposited in the lower section of the building process. Part C was built with a raster motion. Both the water and support material were deposited in this manner for each layer. Part D was built in a way very similar to part A, i.e. with concentric circles being deposited, except that this part was built from the inner circle outwards. Each of these parts were placed in a -5 ° C kerosene bath upon completion and allowed to stay in the bath overnight to remove the support material from the ice structure.

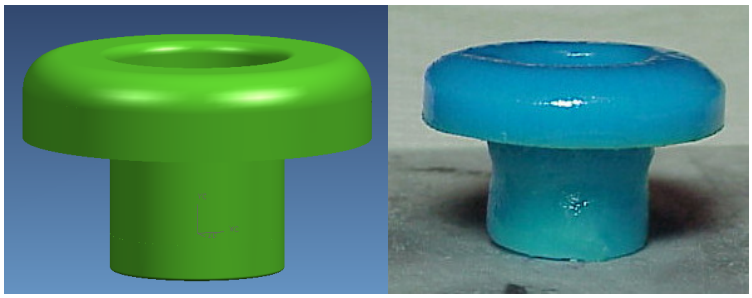

Part A: “Mushroom” ice part CAD model(left) and actual RFP ice part (right)

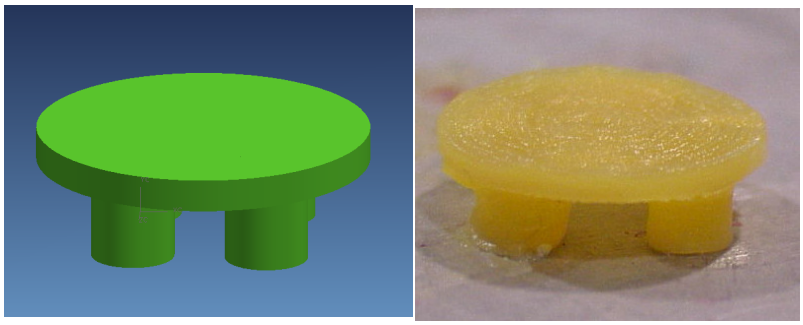

Part B: “Table” ice part CAD model (left) and actual RFP ice part (right)

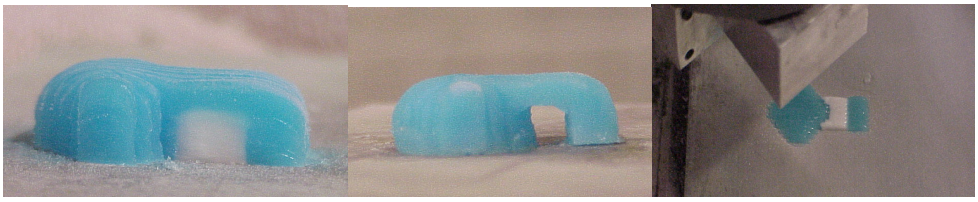

Part C: Ice part with support material (left), after removal (center), and during build (right)

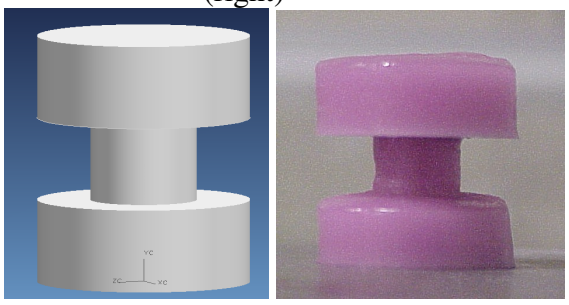

Part D: “Barbell” ice part CAD model (left) and actual RFP ice part (right)

Figure 3.12. Examples of ice parts built with support material

3.5 CONCLUDING REMARKS

A suitable support material has been identified and tested for use in the RFP process. The support material identified is a eutectic dextrose/water ($C_6H_{12}O_6 - H_2O$) solution which is 33% anhydrous dextrose and 67% distilled water by weight. Since a constituent of the support material is water, the support material is water soluble. Diffusion may occur when the support material (dextrose/water solution) and main material (water) are both in liquid states. To minimize the diffusion rate, local cooling has been used in the RFP system to create a colder environment around the deposition region, allowing both water and liquid support material to freeze faster. Ice parts have been fabricated utilizing the local cooling and they exhibit a marked difference at the interface between the main material and the support material. It has been shown through experiments that the rate of diffusion decreases as the ambient temperature decreases. Change in the ice wall height due to the diffusion becomes negligible when the ambient build temperature is lower than -20 ° C.

4. TEMPERATURE MODELING AND VALIDATION

A temperature model which provides insight on the temperature changes occurring during the RFP process has been generated and is described in this section. Predicting the temperature changes occurring during the build process when two materials are being used (i.e. both water and the support material) is crucial to understanding the concentration changes occurring at the interface of the two materials.

4.1 TEMPERATURE MODEL

To determine quantitatively how much mixing or diffusion of sugar from the support material into a newly deposited water layer is occurring, the temperature in the region of interest is investigated first. In order to perform this investigation and to understand the temperature changes occurring during the fabrication process, a two-dimensional temperature model has been developed. For a thin wall of ice and/or support material, a two-dimensional model can be used because heat transfer through the thickness is much less than through the height and width dimensions [Sui and Leu, 2003]. By taking this into account, the temperature at any given location during the fabrication of a thin wall is governed by the following heat conduction equation:

$$\frac{\partial T}{\partial t} = \frac{\lambda}{\rho c}\left(\frac{\partial^2 T}{\partial x^2} + \frac{\partial^2 T}{\partial y^2}\right) + q \qquad (16)$$

where T is the temperature, t is time, x and y are coordinates, q is the internal heat generation, λ is thermal conductivity, ρ is density, and c is specific heat. The values used for water are: λ=0.6 W / m-°C, ρ=1000 kg/m^3 and c = 4174 J / kg-°C. The values used for the support material are: λ=0.6 W / m-°C , ρ=1140 kg/m^3 and c = 2800 J / kg-°C. Since the ice part is built on the top of an aluminum substrate, which is much larger than a thin wall and acts as a heat sink, the temperature at the interface between the

structure and the aluminum substrate can be considered to remain at the ambient temperature, T_{amb}. The initial temperature of the water is denoted as T_{in}. Figure 4.1 represents the model constructed and shows the mesh and boundary conditions. The support material section is shown in white, where the water layer is shown in mid-application in gray.

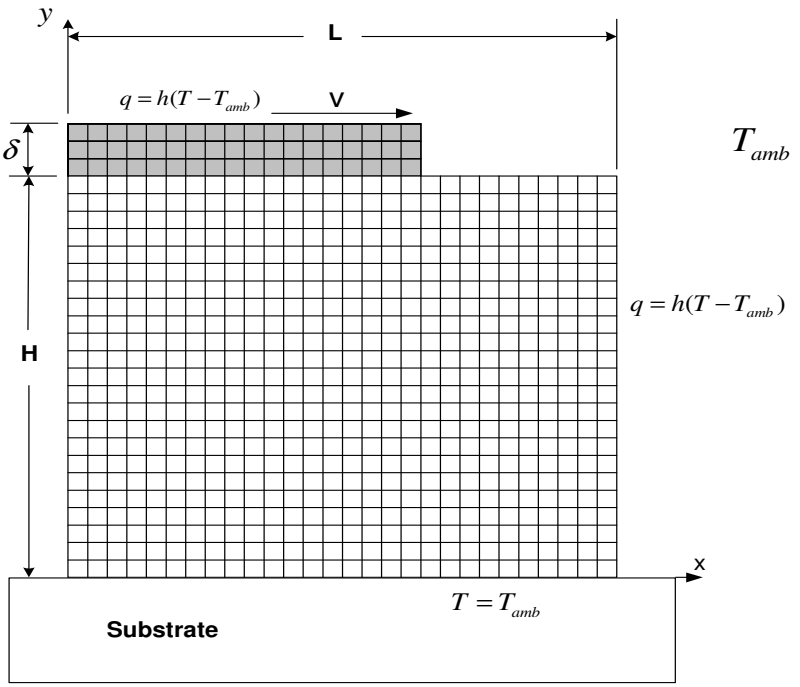

Figure 4.1. Two-dimensional wall of support material (white) and a layer of water (gray) for temperature analysis

The boundary conditions that are applicable to this model and for Equation 16 are:

$$\begin{aligned} &x = 0 \quad 0 \le y \le H \quad t \ge 0 \quad q = h(T - T_{amb}) \\ &x = L \quad 0 \le y \le H \quad t \ge 0 \quad q = h(T - T_{amb}) \\ &y = 0 \quad 0 \le x \le L \quad t \ge 0 \quad T = T_{amb} \\ &y = H \quad 0 \le x \le L \quad t \ge 0 \quad q = h(T - T_{amb}) \end{aligned} \tag{17}$$

and the initial conditions are:

$$0 \le x \le L \quad 0 \le y \le H \qquad t = 0 \quad T(x, y) = T_{amb}$$
$$0 \le x \le L \quad H \le y \le (H + \delta) \quad t = 0 \quad T(x, y) = T_{in} \tag{18}$$

The two sides, x=0 and x=L, have a convective boundary condition, since these edges are exposed to the ambient. The convective heat transfer coefficient used is h = 200 W / m^2-°C, which represents a forced convection situation. The forced convection is due to addition of liquid nitrogen and moving the substrate during fabrication. The upper surface (y=H) of an existing wall is exposed to a convective boundary condition until the new water droplets are deposited upon the existing wall. The new water droplets are deposited at a scan speed v, and modeled as a moving heat source. Finite element analysis is implemented to solve for the temperature at any given time and any coordinates within the wall, using the boundary and initial conditions. The finite element analysis program used in this analysis is ANSYS. Specifically, the Parametric Design Language (APDL) within ANSYS is utilized. The mesh size used is 0.1 mm, whereas a typical water layer height is approximately 0.2 - 0.3 mm.

Since a phase change is involved in this process, the latent heat, which is the energy that the system absorbs or releases during a state change, must be taken into account within the FEA program. The latent heat of the build and support materials is taken into account in the ANSYS/APDL program by defining the enthalpy of each material as a function of temperature [ANSYS, 2004]. The individual element heat capacity during the FEA is evaluated from enthalpy to reflect the phase change.

The ANSYS model used for the temperature prediction represents a moving heat source with a phase change. Figure 4.2 shows an illustrative example of the moving heat source and temperature changes occurring over time within the thin wall model. The deposition of new material is traveling from the left side of the wall to the right side of the wall. The temperature changes in the wall at rates depending on the deposition speed. The lighter areas shown are the warmer areas, whereas the darker areas are cooler. The scan speed shown in the figure is 20 mm/s and the time for each frame is noted underneath the figure. This shows the warming pattern of a thin wall, which is 20 mm in both length and height.

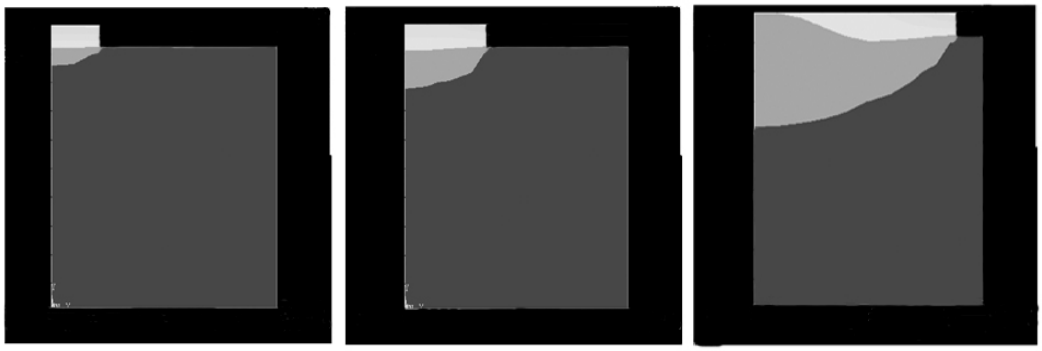

a) t = 0.2 s b) t = 0.4 s c) t = 0.8 s

Figure 4.2. Graphical view of temperature changes in a two-dimensional wall model

4.2 EXPERIMENTAL RESULTS

To verify the results of the temperature prediction model, thin walls were built in the RFP freezer with a length of 20 mm and a height of 10 mm for the support material before depositing water. Beaded wire, T-type thermocouples and a data acquisition board were used with a recording frequency of 5 data readings per second to record temperatures at various locations. The ambient temperature was monitored to insure a

consistent (+/- 1 °C) ambient build temperature during the entire fabrication period. The substrate temperature was also monitored to insure that there were no spikes in temperature. The temperature at the center of the wall at the interface of the two materials was monitored and recorded to compare with the temperature model prediction. The deposited water layer height was 0.2 mm, the wait time between layers was 40 seconds, and the build scan speed was 40 mm/s. Figure 4.3 shows the model temperature predictions for two different ambient temperatures for three water layers applied. The temperature prediction is for the center of the wall at the interface of the support material and water. The three temperature spikes denote the beginning of the new, warm water layer deposition. As shown in the figure, the temperature decreases to the ambient temperature over time before the next warm water layer is deposited. Figure 4.4 shows the predicted temperature for three water layers compared to experimentally measured data in a build ambient of -24 °C.

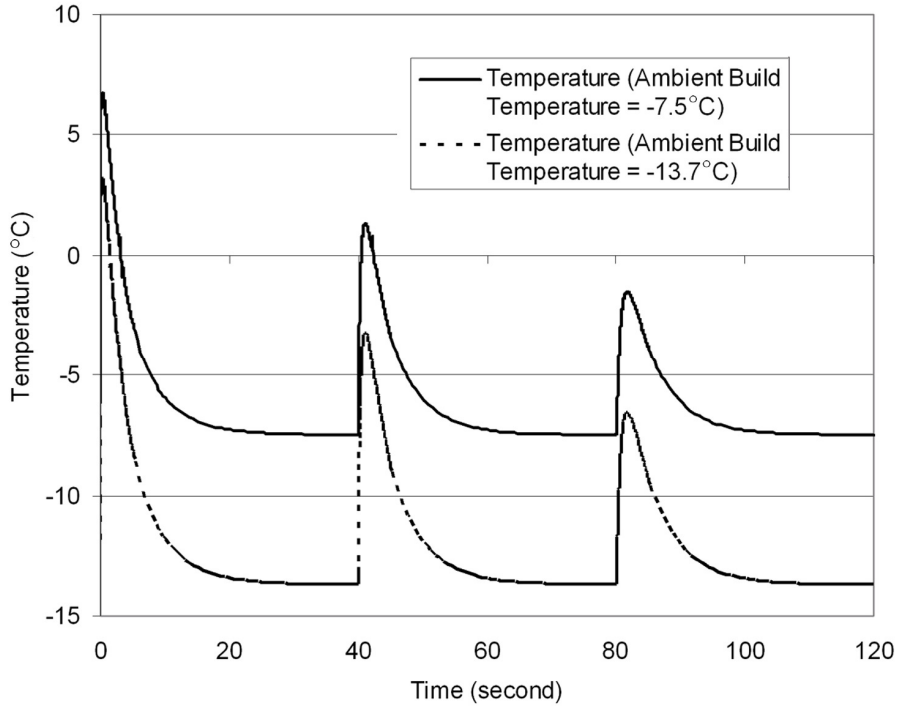

Figure 4.3. Simulated temperature during 3 layer depositions

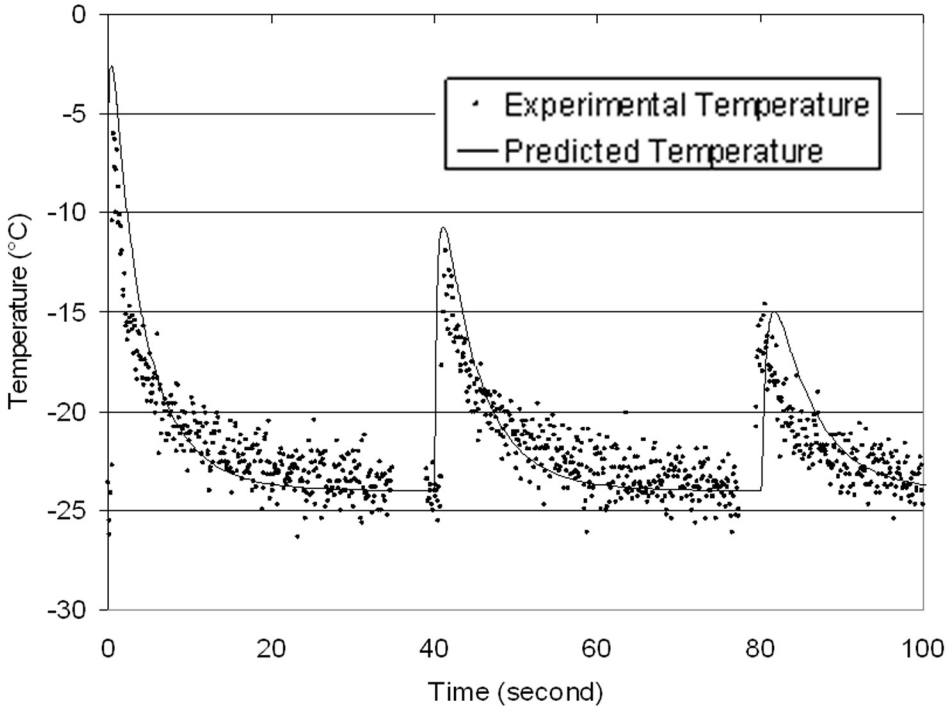

Figure 4.4. Temperature simulation results and experimental data for T_{amb} = -24 °C

The measurements for three different ambient temperatures (-24°C, -13.7°C, and -7.5°C) and comparisons with the model predictions for the first layer of water deposited are shown in Figures 4.5 – 4.7. The experimental data is very challenging to obtain due to embedding the head of the thermocouple into the center of an existing ice structure and having the newly deposited water seal the thermocouple as the new layer freezes. The experimentally collected data also has noticeable electrical noise, which results in scattered data, due to the laboratory environment (i.e. motors, freezers, other machinery, etc.) in which the data was collected.

The temperature prediction model will be used as an input to the concentration model, which will be presented in the next section. If the peak temperature is above 0 °C, then mixing is assumed to be occurring at the interface of the support material and water, since both materials are liquid at temperatures greater than 0 °C. Based on this temperature model, it can be shown from the FEA that if the ambient temperature is less than -19.2 °C, negligible diffusion will occur due to the temperature remaining below 0 °C at the interface. Therefore, there is very little diffusion between newly deposited water and previously deposited and solidified support material if the ambient temperature is less than -19.2 °C.

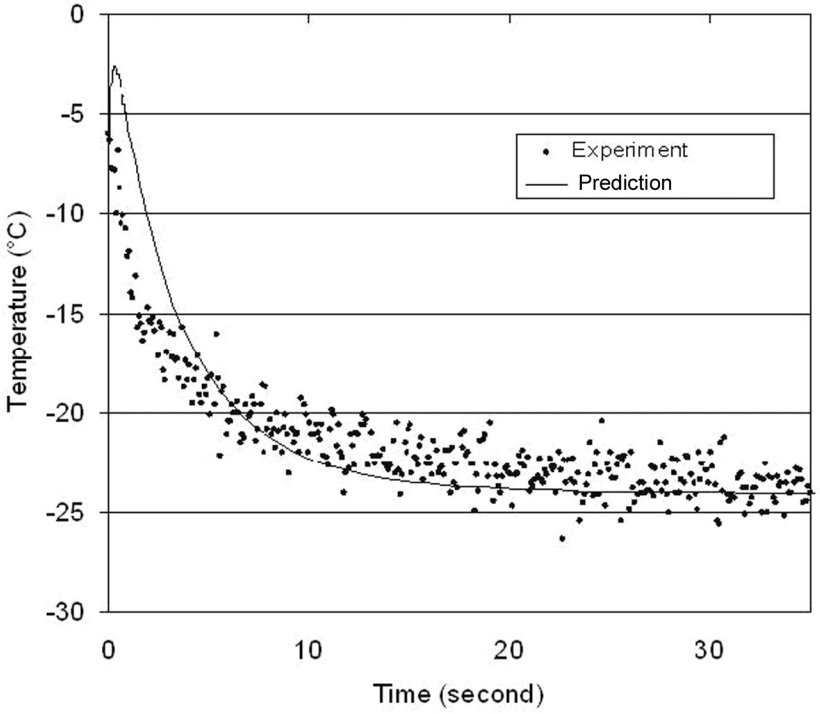

Figure 4.5. Experimental vs. predicted temperature data for an ambient temperature of -24 °C

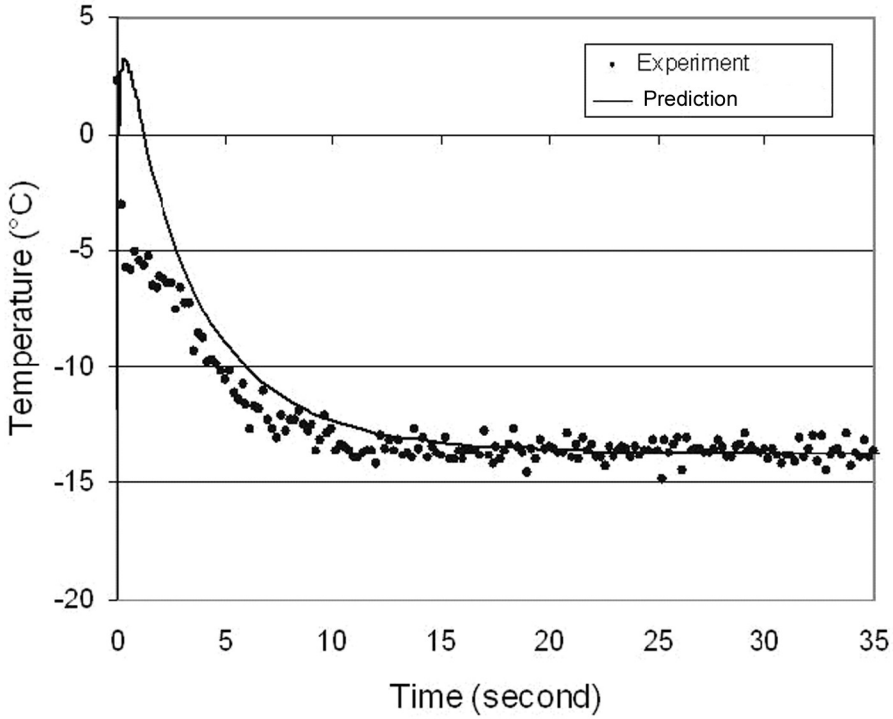

Figure 4.6. Experimental vs. predicted temperature data for an ambient temperature of -13.7 °C

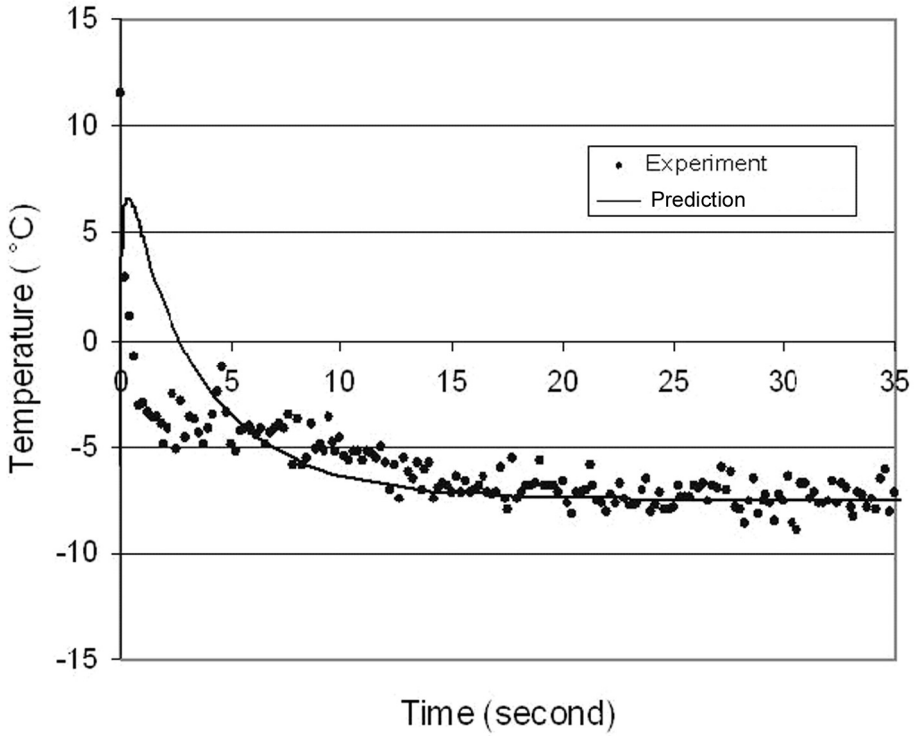

Figure 4.7. Experimental vs. predicted temperature data for an ambient temperature of -7.5 °C

Figure 4.8 shows the highest peak temperature for the first water layer applied as predicted and measured in the RFP setup. This peak temperature is the highest temperature predicted during the simulation of the first water layer deposition and the experimentally measured temperature was recorded with the same thermocouple configuration as noted previously. Each experimentally measured data point represents a single reading.

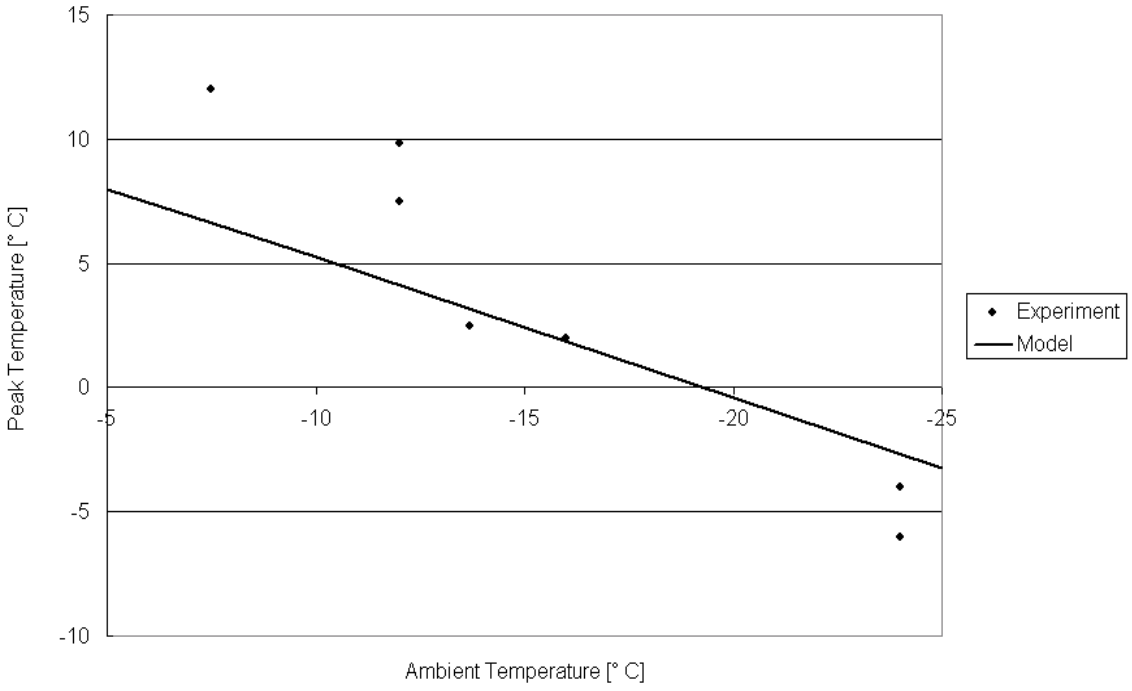

Figure 4.8. Peak temperature during water deposition on support material

4.3 CONCLUDING REMARKS

A temperature model predicting temperature change during ice part fabrication has been developed and compared to experimentally obtained data. The model, which is valid for thin walls, agrees with the experimental data to within a maximum of 6 °C deviation for the first peak temperature (when the first layer of water is deposited onto already frozen support material). The information obtained from this temperature model will be used in the concentration model in the next section to determine the amount of time taken for the interface of the water/ice and support material to alter the concentration of the other material before freezing.

5. CONCENTRATION MODELING

Two models of concentration prediction have been developed and will be discussed in this section. Each model has advantages and disadvantages over the other model. The first model is the continuous concentration model. This model is computationally efficient, but it does not represent the physical process as accurately as the second concentration model, which is the discrete concentration model. The continuous concentration model takes into account a thin wall of support material with a thin wall of water/ice being deposited onto the already frozen wall of support material. This model simulates an 'infinite source' type problem [Crank, 1956]. The entire support material wall area is available for dextrose to diffuse into the entire ice/water wall in this simulation. The time for the diffusion to occur is bounded by the time predicted in the temperature model, where the interface temperature is above the melting temperatures of both materials. This time is less for a lower ambient temperature since the material freezes in a shorter amount of time in a cooler environment. The dextrose will diffuse from the support material area into the water/ice area when both materials are in liquid phase, due to the concentration gradient present. Once the materials freeze, the diffusion is considered negligible and the simulation is considered complete.

The second concentration model presented here is the discrete concentration model. The computation time involved in this model is much longer than that of the continuous model. To compare, the discrete model takes approximately 100 hours to obtain results, while the continuous concentration model can generate results within 10 hours after the relevant data is obtained from the temperature model. Both models were run on a Dell Dimension desktop processor with a Pentium 4 3.2 GHz processor. The

discrete concentration model also considers a thin support material wall. The water layer is deposited on top of the wall of already frozen support material and is implemented in this simulation by the addition of one layer. The initial condition changes for each new layer added in the discrete concentration model. Changing the initial condition each time a layer is deposited dramatically increases the computations required. The two concentration models will be discussed separately and then compared together to experimentally measured data.

For both concentration models, the same basic framework applies. The height 'a' shown in Figure 5.1 denotes the area of degradation in the ice structure where dextrose has migrated, during it's liquid phase, into the water region to cause that region to have enough dextrose such that it is removed in support material removal. The support material area and area 'a' are removed during the support material removal process. Determining the dimension 'a' is the goal of the concentration models, since this dimension represents how much of the ice structure is lost during the support material removal process due to diffusion.

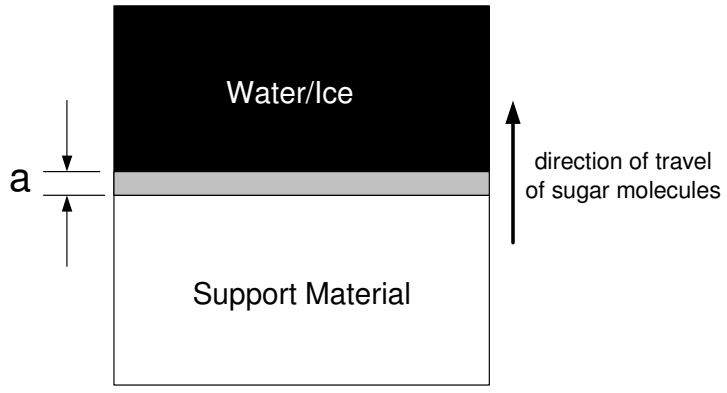

Figure 5.1. Continuous concentration model representation

5.1 CONTINUOUS CONCENTRATION MODEL

In the continuous concentration model, the length of time in which both materials are in liquid phase was obtained from the FEA temperature model. ANSYS/APDL was utilized to obtain numerical results for the continuous concentration model.

The concentration in a thin wall as a function of time and location is governed by the following equation:

$$\frac{\delta C}{\delta t} = -D\left(\frac{\delta^2 C}{\delta x^2} + \frac{\delta^2 C}{\delta y^2}\right) \tag{19}$$

where C is the concentration, D is the diffusion coefficient, t is time, and x and y are spatial coordinates. The concentration model, like the temperature model, has a moving source due to the finite deposition rate.

In order to determine if the moving source will significantly affect the results in the concentration models, a model consisting of one layer of water being deposited onto a wall of already-frozen support material was considered with a moving source. The model considered a 10 mm high wall of support material with a length of 20 mm and a layer of water built upon the support material with a height of 2 mm. Figure 5.2 shows the model dimensions and boundary conditions.

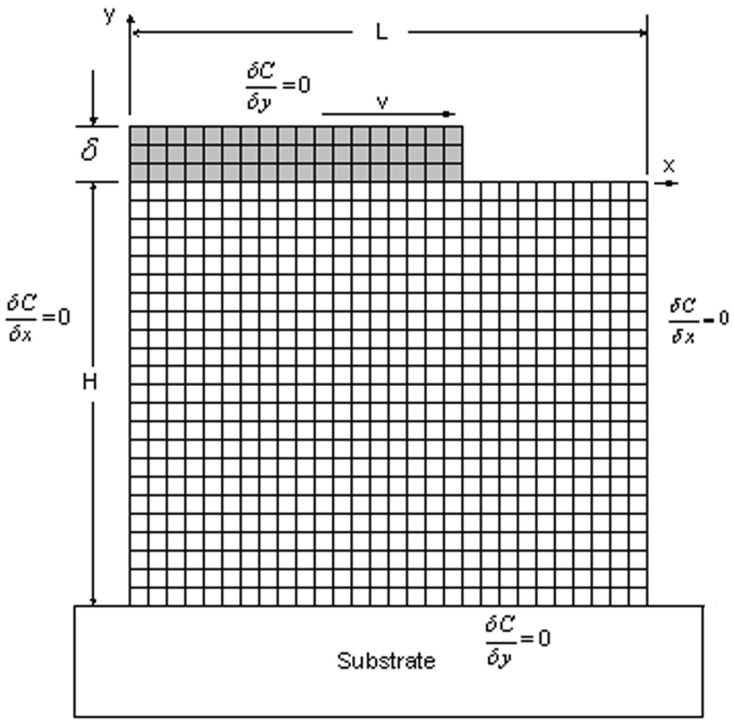

Figure 5.2. Concentration model representation

The boundary conditions for this model are:

$$\begin{aligned} x=0 \quad & -H \le y \le \delta \quad t \ge 0 \quad \frac{\delta C}{\delta x}=0 \\ x=L \quad & -H \le y \le \delta \quad t \ge 0 \quad \frac{\delta C}{\delta x}=0 \\ y=-H \quad & 0 \le x \le L \quad t \ge 0 \quad \frac{\delta C}{\delta y}=0 \\ y=\delta \quad & 0 \le x \le L \quad t \ge 0 \quad \frac{\delta C}{\delta y}=0 \end{aligned} \tag{20}$$

The initial conditions are:

$$\begin{aligned} & 0 \le x \le L \quad 0 \le y \le \delta \quad t=0 \quad C_w(x,y)=0 \\ & 0 \le x \le L \quad -H \le y \le \delta \quad t=0 \quad C_{SM}(x,y)=33 \end{aligned} \tag{21}$$

The two-dimensional concentration model predictions are shown in Figures 5.3 and 5.4.

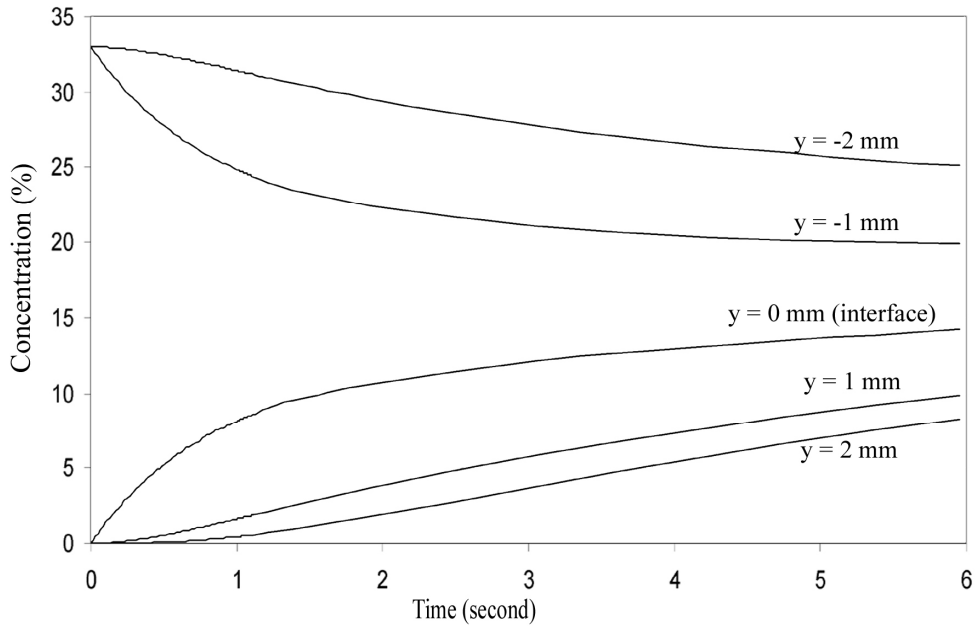

Figure 5.3. Predicted dextrose concentration at different heights in a fabricated thin wall

The dimensions chosen here represent an uncharacteristically large water layer being deposited onto a wall of support material. This simulation was completed to determine if the moving source would considerably change the concentration predictions. The concentration model is simplified if a moving source is not implemented, but the extra computation time is justified if the simulation results vary significantly with and without the moving source.

Figure 5.3 showed the concentration prediction values at various heights in the fabricated wall as a function of time. At the top of the new layer of water

(y = 2 mm) the concentration level is nearer to that of pure water (0 %), whereas at a location lower into the support material (y=-2 mm), the concentration is closer to that of the initial support material concentration (33%).

The results shown in Figure 5.3 consider changes in the y-direction at the transverse center of the wall. There is some potential for concentration changes to occur along the x-axis due to the moving source of deposition. Figure 5.4 shows the predicted concentration along the x-axis (i.e. the nozzle traveling direction).

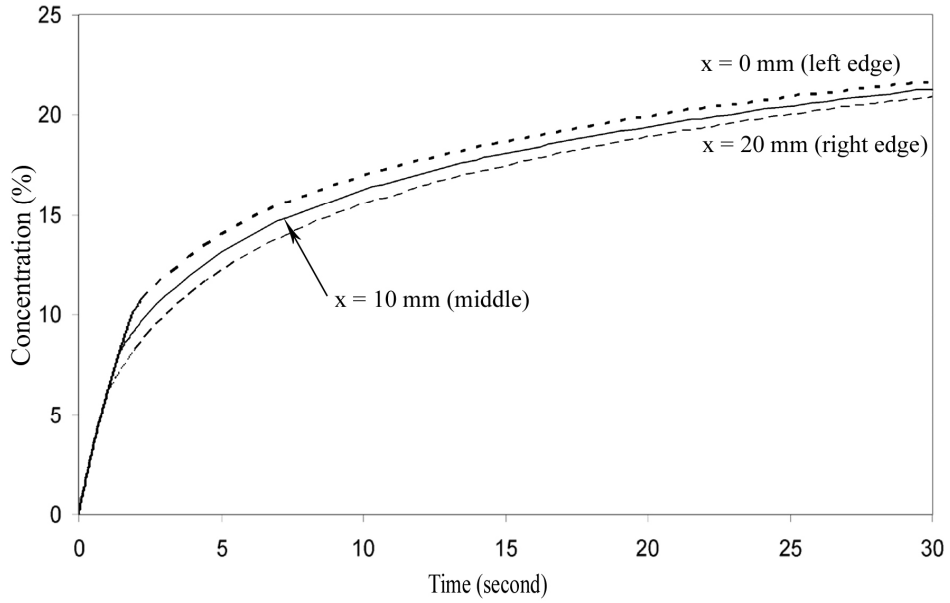

Figure 5.4. Predicted dextrose concentration at different values thru the left edge to the right edge along the x-axis

The values shown in Figure 5.4 are computed with a scan speed of 20 mm/s, which is much smaller than what is typically used in RFP. The small variance that is seen is due to the moving source because of finite deposition rate. The concentration values are within 4% of each other, even at the extreme time of 30 seconds. If the scan speed is slower, the difference in the concentration value along the x direction will be larger. Typically, the scan speed used is 40 - 50 mm/s, so the difference in concentration

along the x-direction in the actual fabrication of a thin wall will be smaller than that shown in Figure 5.4. Since the difference in concentration along the x direction is relatively small, a moving source is not considered necessary to the model and a non-moving boundary is implemented.

Figure 5.5 represents the final continuous concentration model. All outer boundaries are considered to have a concentration flux of zero since diffusion cannot occur across the boundary. The water and support material are in contact at the interface once deposition of the water has occurred. If the temperature of the water (from the temperature model) is above the melting temperature at any time after deposition, diffusion is assumed to occur for the amount of time until the temperature is such that water is frozen.

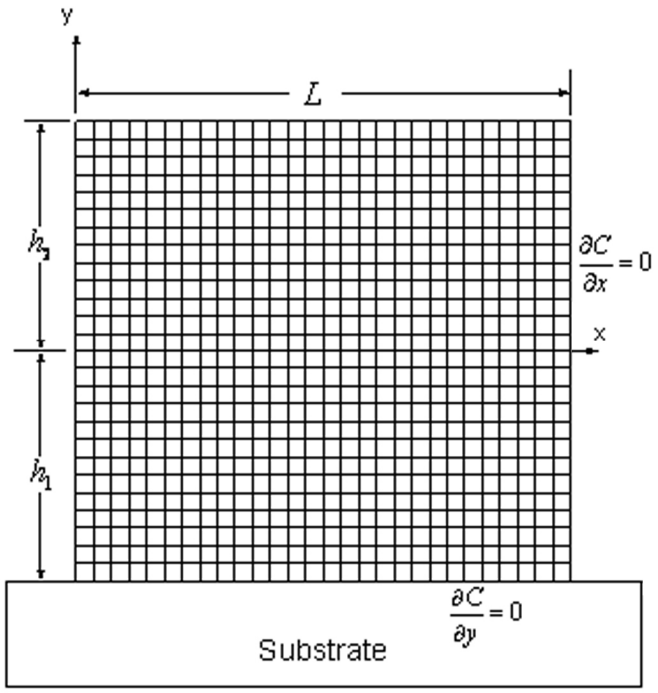

Figure 5.5. FEA concentration model with mesh and boundary conditions

Figure 5.6 shows the results of the continuous concentration model. This plot is based on a 10 mm high wall of support material that is 20 mm in length. A 10 mm high wall of water/ice is deposited onto the already-frozen support material section. A 1% sugar concentration value is used as the cutoff value as to where the ice will be degraded due to diffusion because a reliably used ice wall width value in RFP is 1.2 mm, which corresponds to a 1% sugar concentration for support material removal based on Figure 3.11. The concentration values shown in Figure 5.6 show how the concentration changes over time and along the y axis. For example, the height of the ice wall affected is about 3.5 mm for a freezing time of 5 seconds and is about 5 mm for a freezing time of 10 seconds.

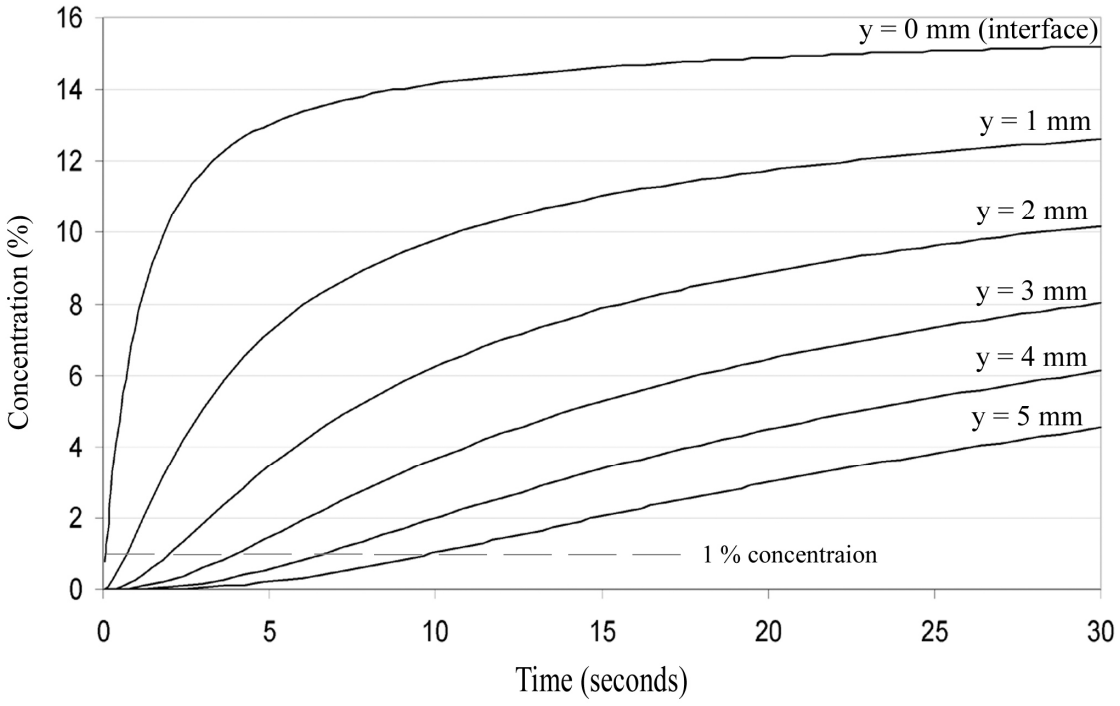

Figure 5.6. Predicted dextrose concentration at different heights along the thin wall

5.2 DISCRETE CONCENTRATION MODEL

The discrete concentration model, which computes concentration changes on a layer-by-layer basis is described in this section. This model is more complex in programming ANSYS for numerical analysis than the continuous concentration model due to the changing initial condition. The initial condition changes because of the mixing of the support and main build materials during the previous layers. Figure 5.7 shows a representation of the discrete concentration model, where δ is the height of the deposited new water layer, ε is the melted depth in the existing wall, and φ is the height of the existing wall with dextrose concentration between 0% and 33%.

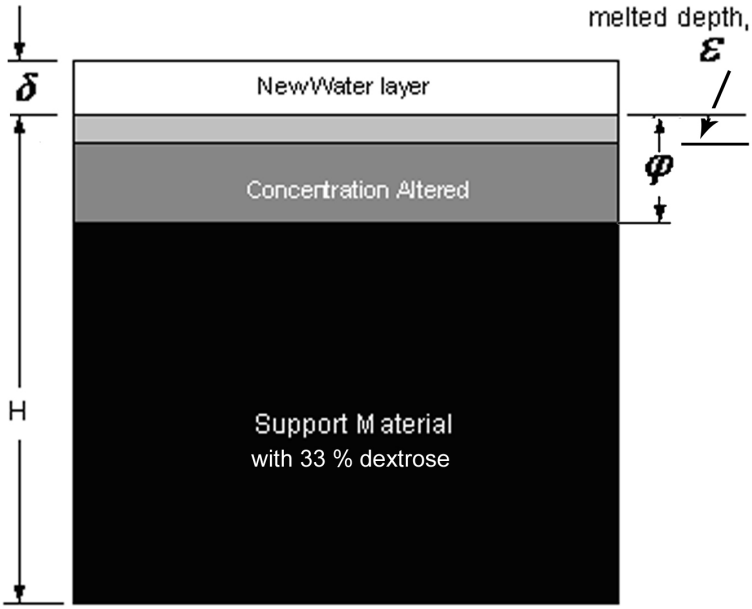

Figure 5.7 Discrete concentration model representation

For the first water layer deposited, φ will have a value of zero, but as layers are deposited, φ will change due to diffusion during the deposition of the previous layers. The melted depth, ε, is the depth of the support material that has been melted and is

available for diffusion. This depth is determined by using the temperature model and calculating to what depth, in the support material section of the wall, the temperature rises to above the freezing temperature of the support material. The melted depth is smaller for lower ambient build temperatures, due to the wall remaining colder and not being affected as much by the layer of warm water being applied.

The governing equation is the same as Equation 19 for the discrete concentration model. The boundary conditions are similar to Equation 20. The only difference is that h_2, shown in Figure 5.5, will be only one deposited layer height. The initial conditions, however, change and are computed each time a new layer is added after the previous layer-added simulation. The concentration varies along the height of the layer after diffusion has occurred. To represent the changing initial conditions, the concentration at the top of each successive new water layer, as predicted in the discrete concentration model, is shown in Figure 5.8 for varying build ambient temperatures. The concentration value shown for each new layer is after the wall has completely frozen and diffusion has 'stopped' until the next layer is added.

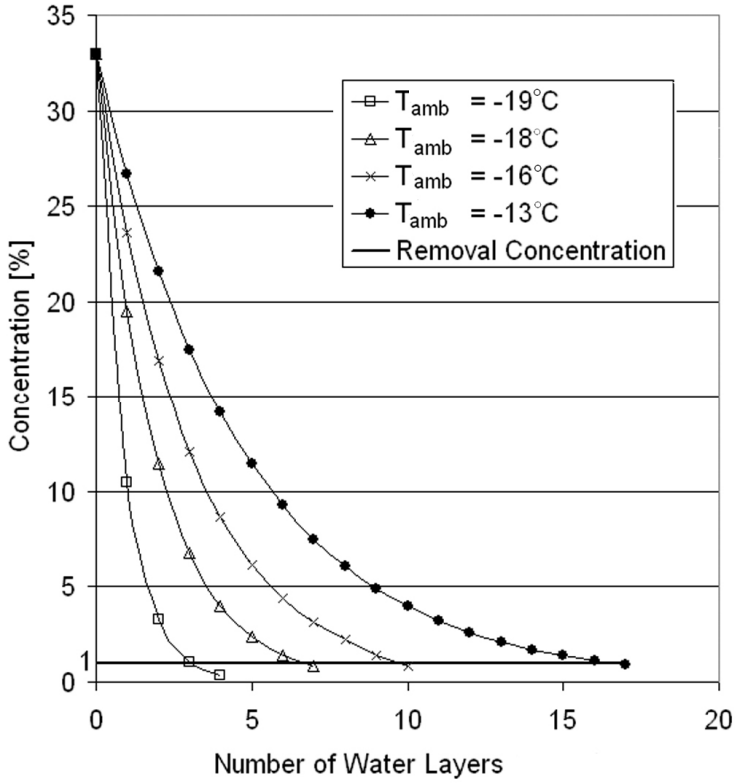

Figure 5.8. Top layer concentrations for varying ambient build temperatures

The first point for each curve in Figure 5.8 is 33%, which is the concentration of the support material. The next point in each curve is the concentration at the top of the first deposited water layer, the third point is the concentration at the top of the second deposited water layer, and so on. The model is run until the top layer concentration is < 1% dextrose. The 1% concentration value comes from Figure 3.11, which represents a concentration threshold for support removal for a typical build wall thickness of 1.2 mm.

5.3 EXPERIMENTAL RESULTS

In order to compare simulation results of both concentration models with experimental data, thin walls of support material as the lower section and ice/water as the upper section were fabricated in varying ambient temperatures. The walls had lengths of

20 mm and heights of 10 mm each and a thickness of 1.2 mm. The design dimensions for the test walls are shown in Figure 5.9. The fabricated walls were transferred to a kerosene bath at a temperature of -5 °C and agitated to remove the support material. Figure 5.10 shows an example of a fabricated test wall, as well as a close-up picture of an area affected by diffusion in this wall.

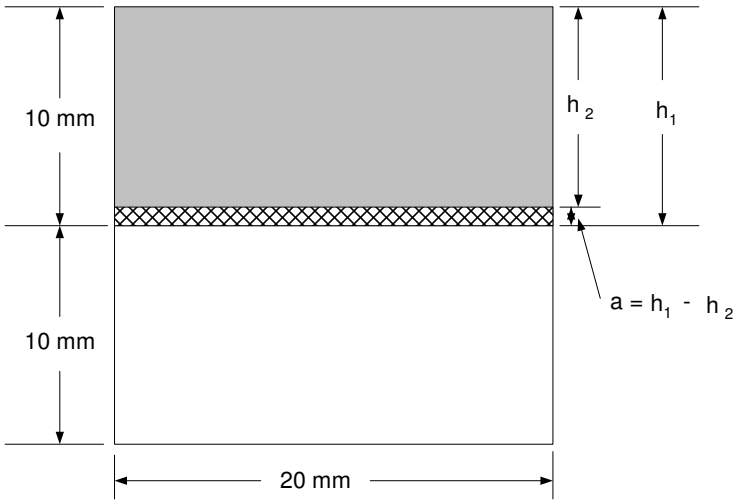

Figure 5.9. Experimental wall dimensions

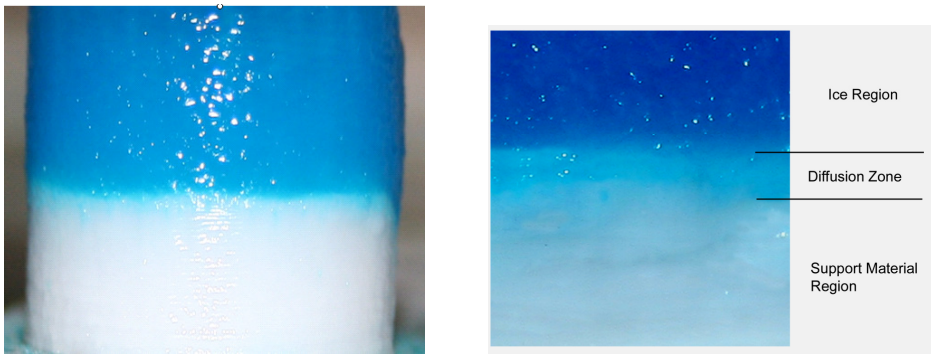

(a) (b)

Figure 5.10. Fabricated test walls with 2 different scenarios: a) no diffusion, and b) significant diffusion

The concentration models were used to predict how much of the ice wall would be degraded due to diffusion of dextrose from the support material region to the water/ice region near the interface for varying ambient temperatures. Table 5.1 compares the experimental data with the predictions from each concentration model. The ambient temperature given is the environment temperature at which the walls were fabricated.

Table 5.1. Comparison of height data for ice parts built in varying ambient temperatures after support material removal, where T_{amb}=ambient build temperature, $t_{diffusion}$ = time during which diffusion occurs, $h_{,pred,cont}$ = predicted wall height for continuous concentration model, $h_{,pred,\ disc.}$ =predicted wall height for discrete concentration model, and $h_{measured}$ = average measured wall height after support material removal

T_{amb}	$t_{diffusion}$	Continuous Model $h_{,pred,cont}$ [mm]	Discrete Model $h_{,pred,\ disc.}$ [mm]	$h_{measured}$	% Diff. Cont.	% Diff. Disc.
-13	1.3	8.45	8.30	7.79	5.68	3.97
-15	0.96	8.72	8.58	8.30	4.82	3.26
-16	0.81	8.80	8.71	8.65	1.70	0.69
-18	0.47	9.14	9.08	9.47	-3.6	-4.99
-19	0.22	9.60	9.50	9.67	-0.73	-1.79
-20	0	10	10	9.98	0.2	0.2
-21	0	10	10	10.05	-0.5	-0.5
-22	0	10	10	9.96	0.4	0.4

Figure 5.11 shows the height difference (nominal build height minus height removed due to diffusion, or ‘a’ in Figure 5.9) as predicted from both the continuous and discrete concentration models, and the measured experimental data.

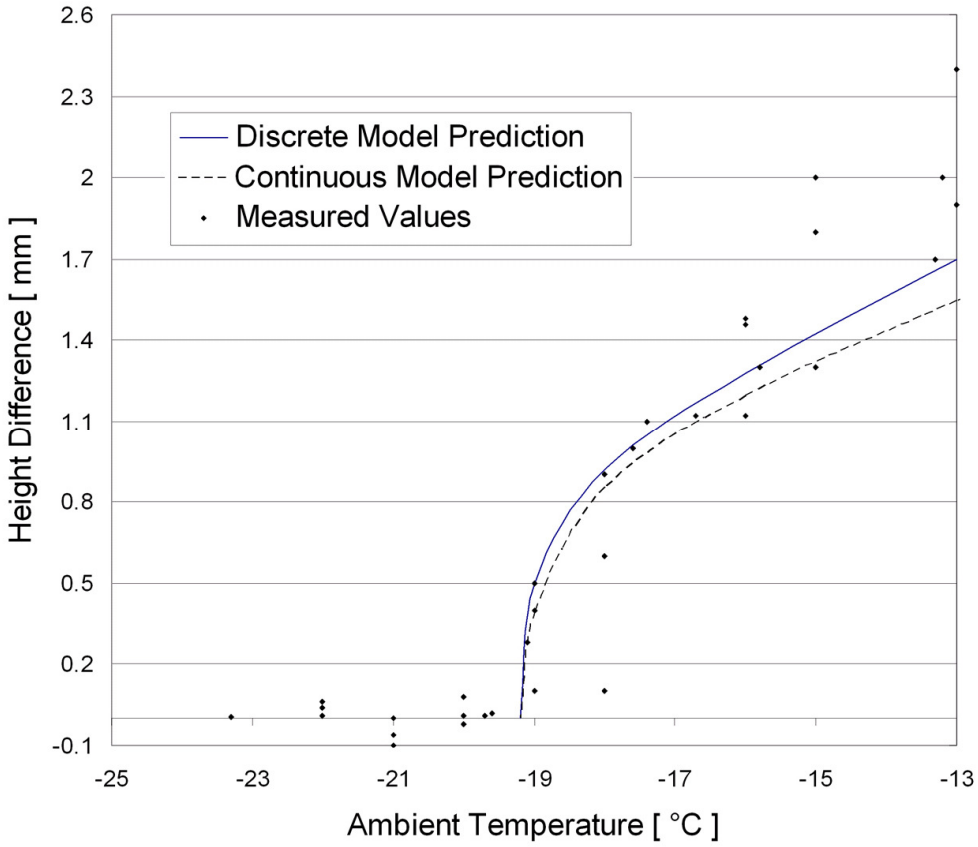

Figure 5.11. Discrete and continuous concentration model results compared to experimental data

Figure 5.12 shows a fabricated ice part which requires support. The part shown in this figure was built in an ambient of -8.5 °C. Clearly, there is severe diffusion occurring at the interface between the water/ice and support material. Figure 5.13 shows a designed part and the corresponding fabricated part, both before and after support material removal. The part was built in an ambient of -23° C. It has a sharper boundary at the interface of water/ice and support material compared with the part built at -8.5 °C, as expected. Figure 5.14 shows another ice part with an overhang feature and the fabricated part, before and after support material removal. Figure 5.15 shows a fabricated ice part with a supported center section. The left side of the figure shows the bridge-type section

as fabricated with the support material still in the structure. The right hand side of the figure shows the part after the center supported region has been removed.

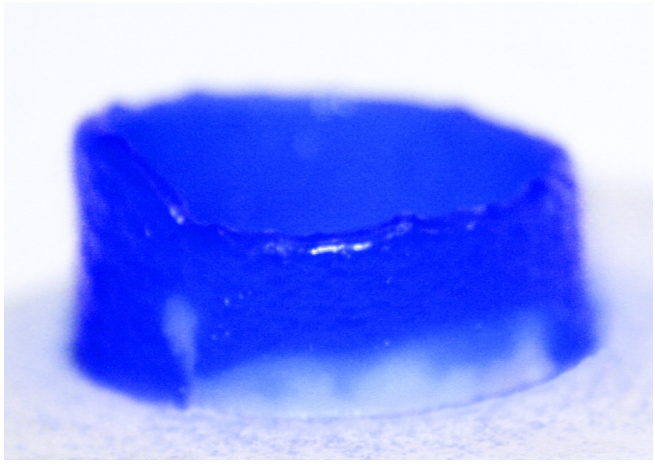

Figure 5.12. Cylinder shell ice part with support region (white) built in -8.5 °C ambient

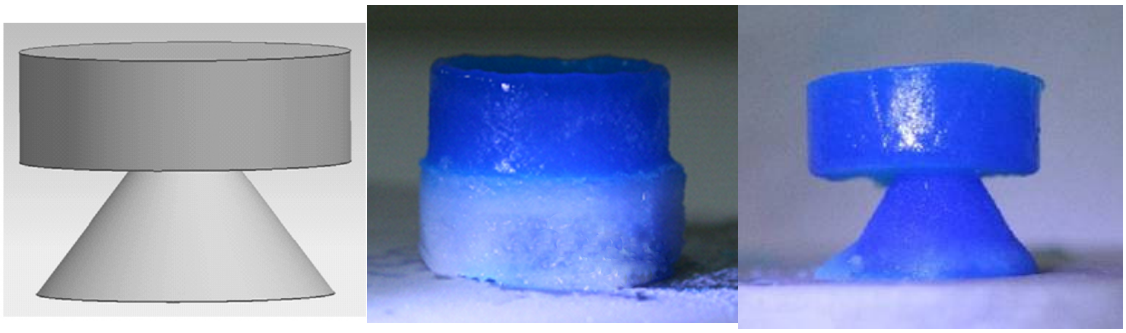

Figure 5.13. An ice part built in -23 °C ambient: (a) CAD model, (b) before support material removal and (c) after support material removal

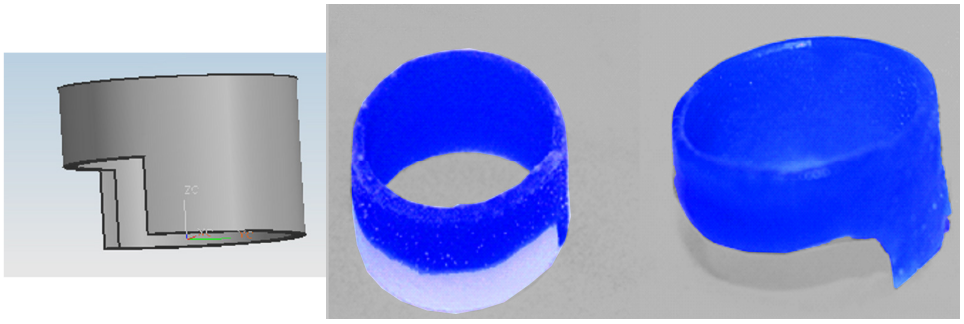

Figure 5.14. A cylinder built in -23° C ambient: (a) CAD model, b) before support material removal and (c) after support material removal

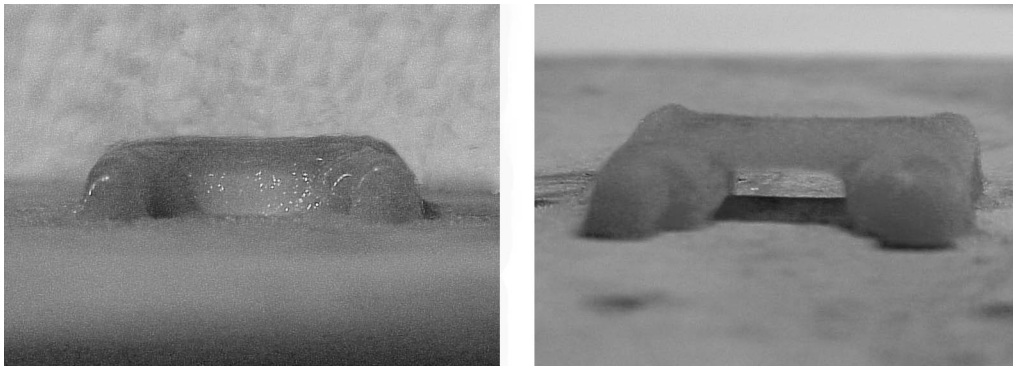

(a) (b)

Figure 5.15. A fabricated ice part with a supported center section: (a) before support material removal and (b) after support material removal

5.4 CONCLUDING REMARKS

Two models, one continuous model and one discrete model, have been presented for concentration analysis. Each model has been described and compared to experimentally measured data. The continuous concentration model has more simplifications and assumptions than the discrete concentration model. This makes the continuous concentration model more computationally efficient. The discrete concentration model more closely replicates the physical process occurring during fabrication in RFP. This comes with a high computation cost, however. For thin walls, the experimental data closely matched the predictions of both concentration models to within 6% for height dimensions of a designed ice wall. Depending on the tolerances allowed, using a continuous concentration model could provide close enough approximations if computation time were a main concern. Both concentration models predict the same trend, where an ice structure is compromised more when built in a warmer ambient. This trend and quantitative predictions were also verified with experimentally measured data.

6. DIMENSIONAL ACCURACY AND SURFACE ROUGHNESS

How to consistently build ice parts which are dimensionally accurate is considered in this section. The surface roughness of ice parts is also studied. Being able to construct ice parts with smooth surface roughness and to close tolerances is necessary for acceptance of parts built by RFP and is addressed in this section.

6.1 DIMENSIONAL ACCURACY OF ICE PARTS

The current RFP setup lends itself to creating ice lines with circular arc paths due to the ramp-up acceleration of the X-Y positioning system embedded in the system's software. The system also builds parts without corners more accurately due to the system being open-loop, not being able to detect and compensate for inconsistencies in the ice lines. Since using arc paths during ice part fabrication inherently creates a better ice part in the RFP setup, a cylinder was designed and built for studying the dimensional accuracy of ice parts. The designed cylinder part used in this study is shown in Figure 6.1.

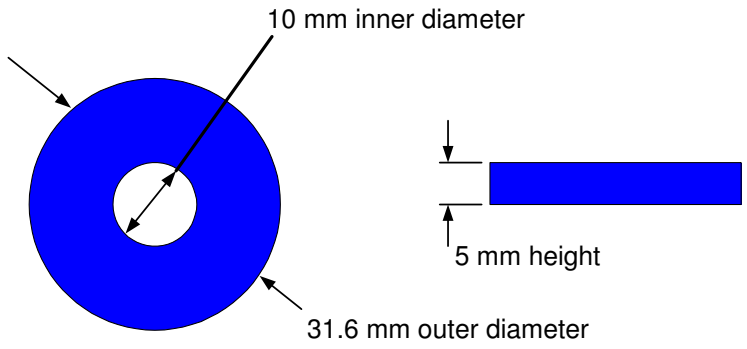

Figure 6.1. Test cylinder design dimensions

A line width of 1.20 mm was chosen for this study, as this dimension can be reliably used for the fabrication. The outer cylinder diameter of 31.6 mm is chosen based

on the line width, with 9 concentric circles needed to create each layer of the cylinder. In order to deposit the material to create the desired dimensions of the cylinder, path planning was performed. A line of water has the appearance as shown in Figure 6.2, which is semi-capsule in shape. A line of support material has the same appearance.

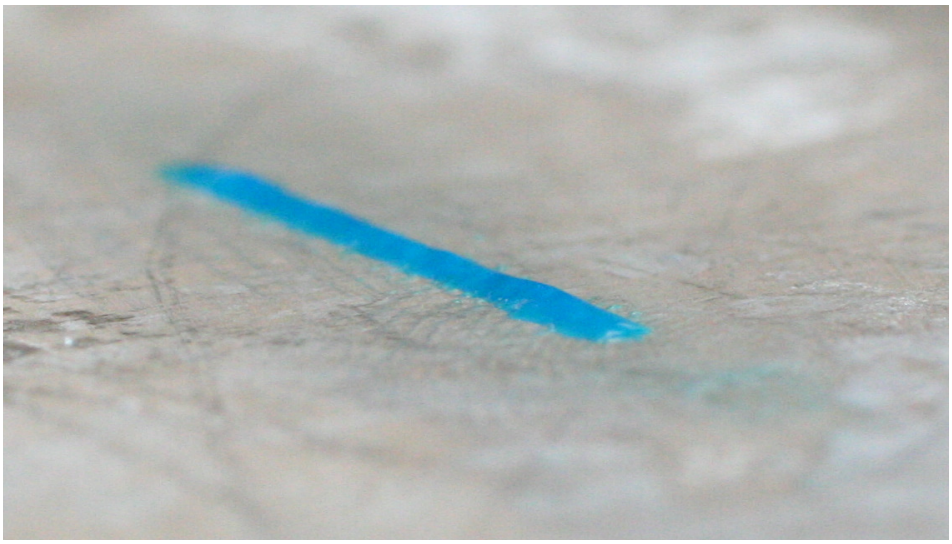

Figure 6.2. A single ice line

To create solid cylinders, circular paths were planned to be adjacent to each other, but not overlap. It was observed in solid ice parts that excess build-up is accrued in each layer if overlap between ice lines is programmed into the path of the nozzle. In this case, the cylinder could have either a convex or a concave top surface, depending on the build direction for each layer. If the outer portion of the cylinder is deposited first and the nozzle continues inward to create the solid cylinder, the cylinder will have a convex appearance on the top surface, as shown in Figure 6.3. However, if the inner portion is deposited first in each layer and the nozzle proceeds outward, the cylinder will have a convex appearance on the top surface, as shown in Figure 6.4.

Figure 6.3. A cylinder built from the outside moving inward for each layer with excessive build-up

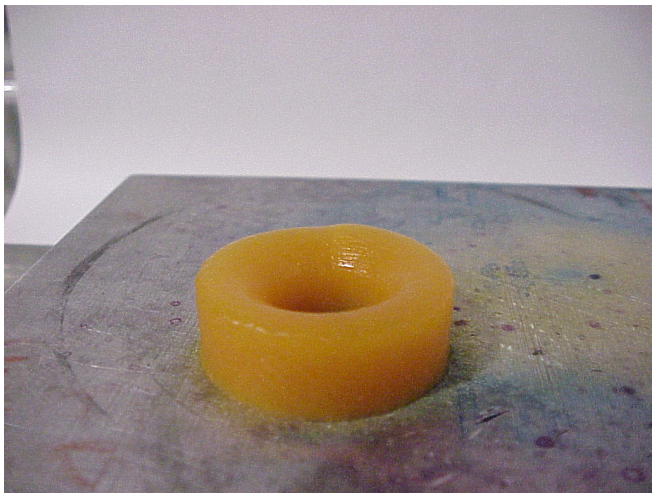

Figure 6.4. A cylinder built from the inside moving outward for each layer with excessive build-up

The nozzle path for the test cylinders, which are designed to have a flat upper surface, is shown in Figure 6.5. The nozzle starts at the origin, travels along the dashed arc and starts deposition at the 'X'. A circle path is followed with the nozzle depositing material until the nozzle returns to 'X', at that point the nozzle turns off and another arc is traveled back to the origin. This process is repeated until enough material has been

deposited to create a complete cross-section of the cylinder. The arc-shaped paths ensure that acceleration/deceleration of the XY-table will not create any excess material or build-up in the finished ice part.

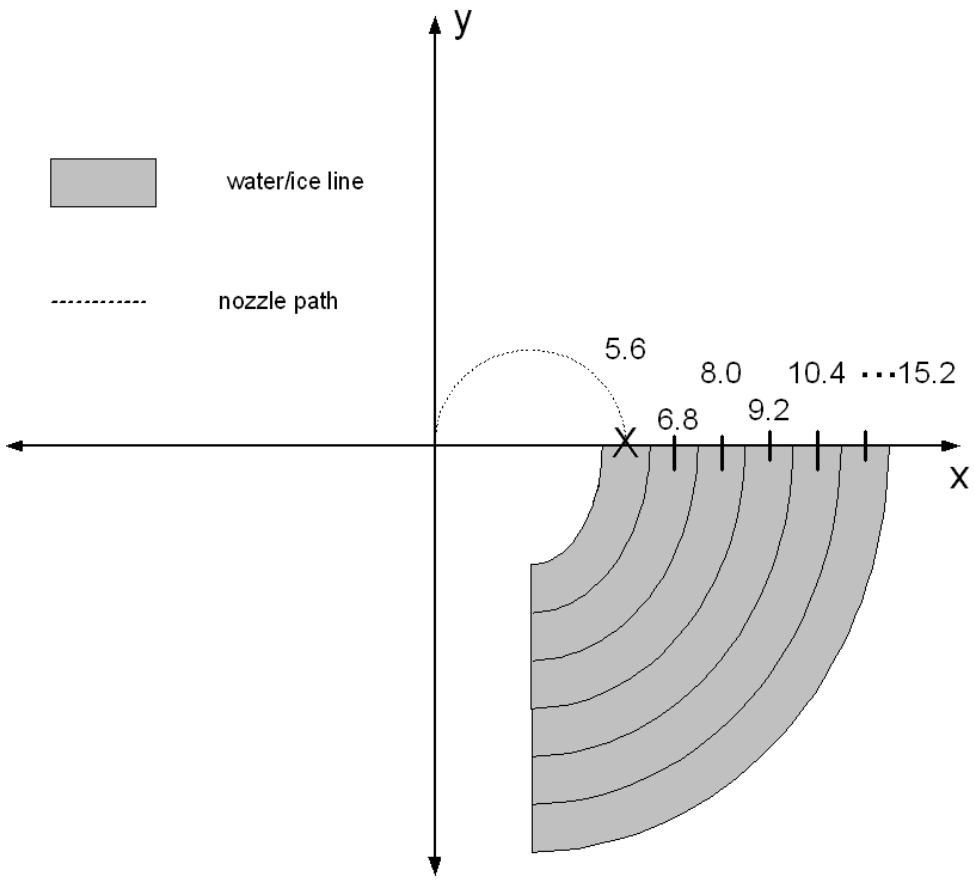

Figure 6.5. Nozzle path for creating accurate cylinders

The dimensional accuracy study performed here considered four cases given in Table 6.1.

Table 6.1. Build parameters for test cylinders

Case	Ambient Temperature	Use of Support Material
1	-18 °C	No
2	-22 °C	No
3	-18 °C	Yes
4	-22 °C	Yes

The reason -18 °C and -22 °C ambient temperatures were chosen is because, based on the concentration models already discussed, -18 °C should have measurable diffusion occurring, whereas -22 °C should have negligible diffusion. For cases 3 and 4, the support material was deposited first for each layer, followed by water. This was done so that the amount of ice structure lost by diffusion from the center support material section to the ice section could be predicted by the concentration models discussed in Section 5. Based on the build temperatures, case 4 should not have a measurable degradation in the ice, because the build temperature is low enough to prevent significant diffusion. For case 3, however, the concentration models predict that there will be a measurable amount of ice lost. A summary of each build case, along with the predicted final dimensions and measured dimensions, for the cylinders is given in Table 6.2.

Table 6.2. Build parameters, predicted and measured dimensions for test cylinders

Case	T_{amb}	Support Material	Nom. inner dia. [mm]	Inner diameter predicted Cont./Disc. [mm]	Inner dia. meas. [mm]	Nom. outer dia. [mm]	Outer dia. meas. [mm]	Nom. height [mm]	Height meas. [mm]
1	-18	No	10.0	10.0	10.0	31.6	31.6	5.0	5.0
1	-18	No	10.0	10.0	9.99	31.6	31.7	5.0	5.0
1	-18	No	10.0	10.0	9.98	31.6	31.6	5.0	5.1
Avg.	—	—	—	—	9.99	—	31.63	—	5.03
2	-22	No	10.0	10.0	9.97	31.6	31.3	5.0	5.2
2	-22	No	10.0	10.0	10.0	31.6	31.4	5.0	5.2
2	-22	No	10.0	10.0	9.99	31.6	31.5	5.0	5.1
Avg.	—	—	—	—	9.99	—	31.40	—	5.17
3	-18	Yes	10.0	11.72/11.84	11.4	31.6	31.6	5.0	5.0
3	-18	Yes	10.0	11.72/11.84	11.35	31.6	31.4	5.0	5.2
3	-18	Yes	10.0	11.72/11.84	11.2	31.6	31.4	5.0	5.1
3	-18	Yes	10.0	11.72/11.84	11.3	31.6	31.5	5.0	5.1
Avg.	—	—	—	—	11.31	—	31.48	—	5.10
4	-22	Yes	10.0	10.0	9.98	31.6	31.5	5.0	5.1
4	-22	Yes	10.0	10.0	10.0	31.6	31.5	5.0	5.0
4	-22	Yes	10.0	10.0	9.99	31.6	31.6	5.0	5.0
Avg.	—	—	—	—	9.99	—	31.53	—	5.03

It can be seen from Table 6.2 that in the cases where the support material was not used (cases 1 and 2) and also the case where the support material was used in a -22 °C ambient (case 4) there is negligible ice lost based on the inner diameter measurement. For case 3, where the support material was used in the center portion in order to make a

hole, the inner diameter increases for the final dimension. The amount of change in diameter was overestimated by the concentration models. This is most likely due to the fact that the cylinders are solid parts while the concentration models presented for finite element analysis were for thin wall structures. The average measured inner diameter compared to the prediction from the continuous concentration model has a difference of 3.5% and compared to the prediction from the discrete concentration model has a difference of 4.5%.

Figures 6.6 – 6.9 show some of the ice cylinders built in the dimensional accuracy study. Different features are noted for each photograph. Each photo shows a different aspect of the cylinder. A completed cylinder, built with case 1 conditions (-18 °C ambient with no support material used), is shown in Figure 6.6. Figure 6.7 shows a cylinder for case 3, i.e. built in -18 °C with support material during fabrication. The water and support material nozzles are inside the deposition head shown in the picture. Figure 6.8 shows the completed cylinder with an inner cylinder of support material before removal of the support material. Figure 6.9 shows a cylinder, with support material in the center, where the top and side surfaces can be seen before the support material removal.

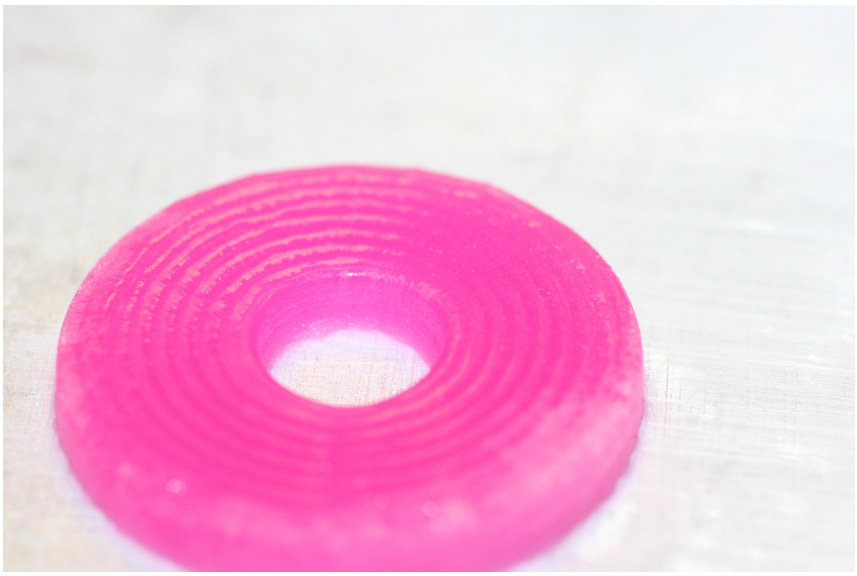

Figure 6.6. An ice cylinder built in -18 °C ambient

Figure 6.7. An ice cylinder with support material during fabrication

Figure 6.8. A completed ice cylinder with support material

Figure 6.9. Top and side surfaces of a completed ice cylinder

Figure 6.10 shows the cylinder during the support material removal. A loose piece of support material can be seen directly left of the cylinder, while more support material can still be seen in the inner diameter of the cylinder. The solid support material breaks off in pieces during the agitation in the kerosene bath. Figure 6.11 shows the bottom surface of a cylinder after support material removal. Figure 6.12 shows the top surface of a cylinder after support material removal. The top portion of the photo has glare due to some kerosene remaining on the ice part, whereas the lines of deposition can clearly be seen in the bottom portion of the photo. Figure 6.13 shows a side view of the cylinder after support material removal. The top level can be seen to be fairly level. Figure 6.14 show the measurement of outer diameter with a caliper.

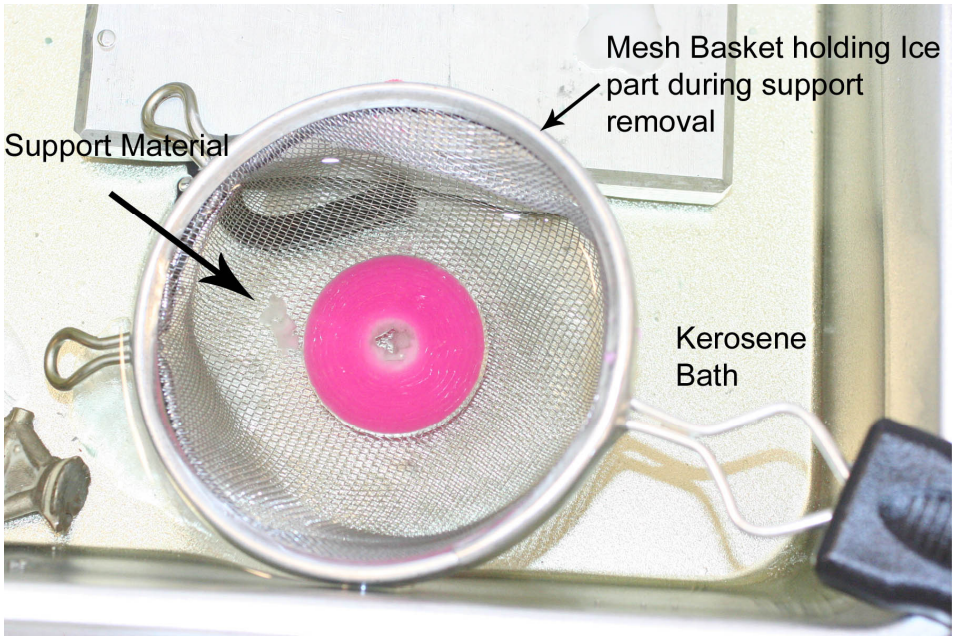

Figure 6.10. An ice cylinder with support during support material removal

Figure 6.11. Lower surface of an ice cylinder after support material removal

Figure 6.12. Upper surface of an ice cylinder after support material removal

Figure 6.13. Side view of a completed ice cylinder

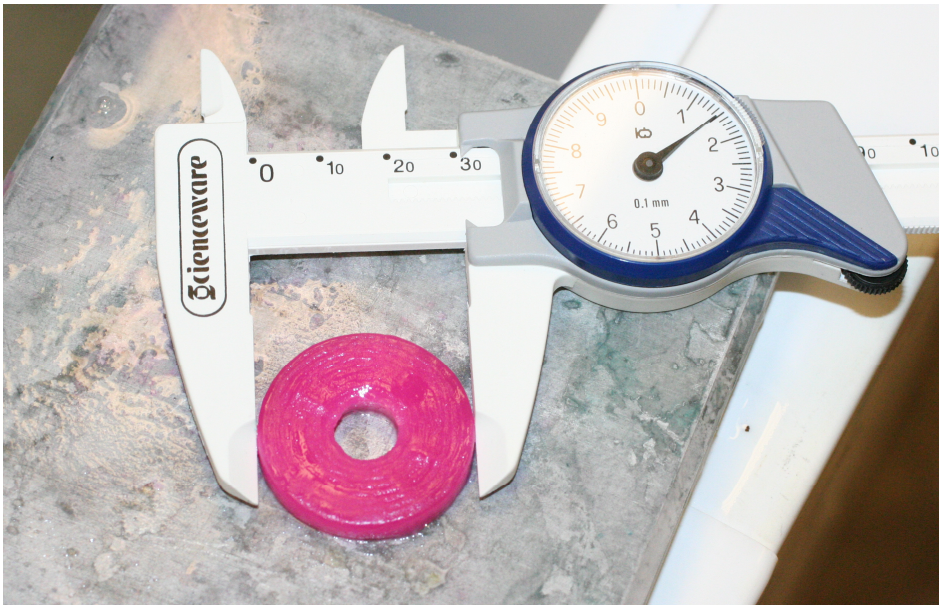

Figure 6.14. Measurement of outer diameter of an ice cylinder

6.2. SURFACE ROUGHNESS

The surface roughness of ice parts has been measured for the side surfaces of fabricated ice parts [[b]Sui, 2002]. The surface roughness is an arithmetic average of the measure of the deviations in surface valleys and peaks. Measuring the top surfaces of solid ice parts and areas where support material has been removed is considered here. The surface roughness was measured for ice parts by using silicone copies of the ice parts. Dow Corning 3110 RTV Silicone Rubber Encapsulant was used along with Dow Corning 4 catalyst to cure the silicone mold. The silicone and catalyst was stored in the RFP freezer so that the temperature of the molding material remained low enough to not melt any features of the ice parts. Dow Corning 3110 can be used in temperatures as low as -55 °C. Ice parts were fabricated and then silicone, mixed with the catalyst, was poured over the parts to create the negative pattern. The silicone was allowed to cure over 24 hours and then a Mitutoyo Surftest SJ-201P surface roughness tester was used to measure the surface roughness of the ice parts in various locations.

For the cylinders used in the dimensional accuracy study, the average surface roughness measurement of the top of the ice part (where no support material was in contact with water/ice) was 3.4 micron. To test the surface roughness of ice where support material had previously been deposited and then removed, ice cylinders were built on a planar support material base. The base plane of support material was then removed after depositing and freezing water droplets to build a cylinder. The ice part remaining was used as the pattern to create a silicone mold. The area where ice had been in contact with support material was measured and the average surface roughness is 1.26 micron. A mushroom shaped part was also used as a pattern for a mold and the

underneath side of the upper section was measured for surface roughness. The surface roughness of this location measured an average of 2.6 micron. A table showing the location of each type of measurement is shown in Table 6.3. The surface roughness values, the mean and standard deviations of the measurements are given in Table 6.4.

Table 6.3. Surface roughness measurement locations

Case	Type of Surface on which surface roughness is measured	Measurement Location
I	Ice Surface (no support material used)	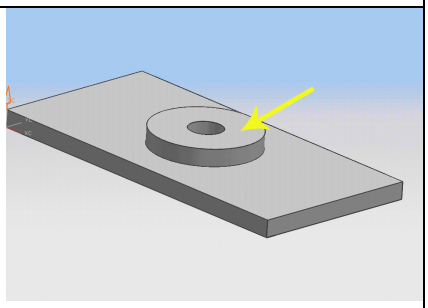
II	Ice surface built on support material (after support material removal)	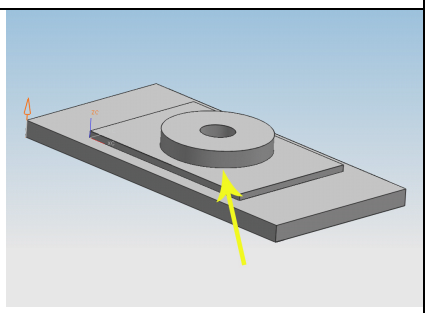
III	Lower Ice face of mushroom section	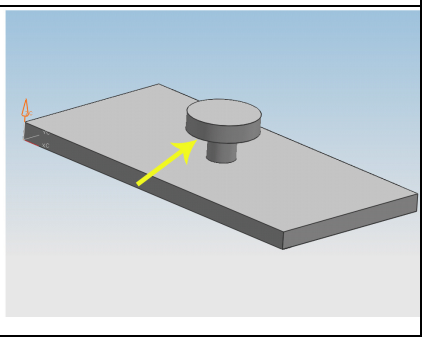

Table 6.4: Surface roughness values, mean and standard deviation

Measurement	Case I	Case II	Case III
1	3.2	0.83	2.6
2	3.5	0.85	3.0
3	3.1	0.86	2.7
4	3.6	0.87	2.4
5	4.1	1.5	2.4
6	3.2	1.62	2.9
7	3.4	1.75	2.3
8	3.3	1.78	2.5
Mean	3.4	1.26	2.6
Std. Deviation	0.32	0.44	0.25

6.3 ICE PARTS FABRICATED

Solid ice parts have been created at the conclusion of this study in order to show that the process can build complex parts out of ice with use of support sections. Some of these parts are shown in the photos in Figures 6.15 – 6.28. The information obtained from the study of temperature changes and concentration changes during fabrication was used in the fabrication of these parts as to decrease diffusion as much as possible during the fabrication time. The lower area of the 'mushroom' part seen in Figure 6.15 has noticeably straighter edges than in previously built supported ice parts that were shown earlier.

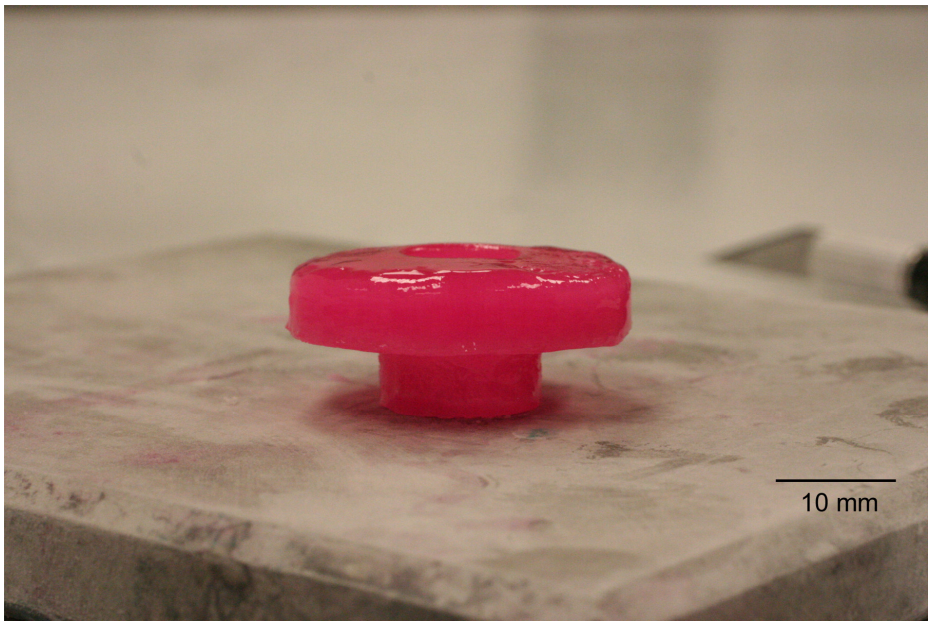

(a)

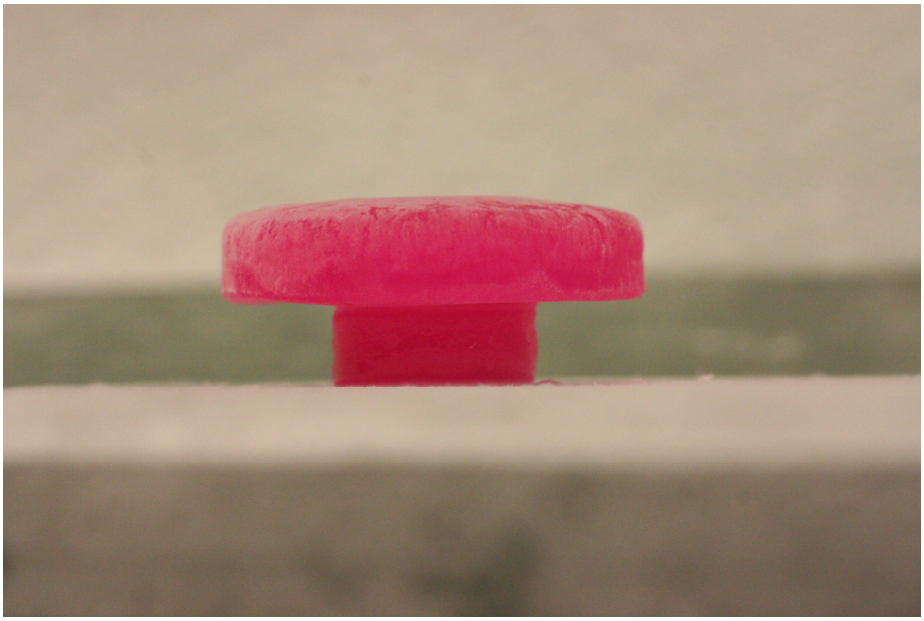

(b)

Figure 6.15. Two views of ‘mushroom’ ice part after support material removal

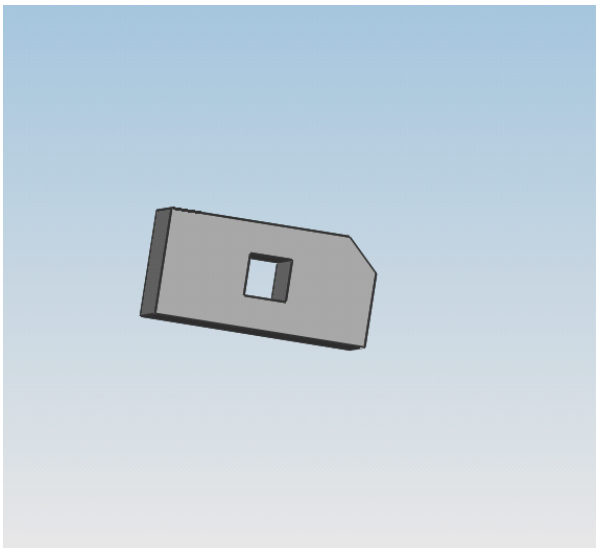

(a)

(b)

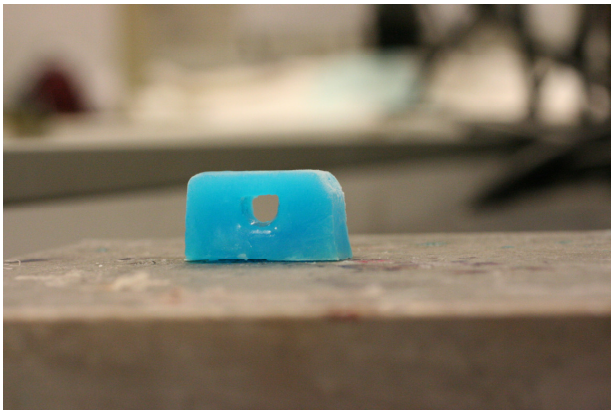

(c)

Figure 6.16. CAD model of a 20 mm long ice block with a square hole (a), ice block with supported interior section (b), and ice block after support material removal (c)

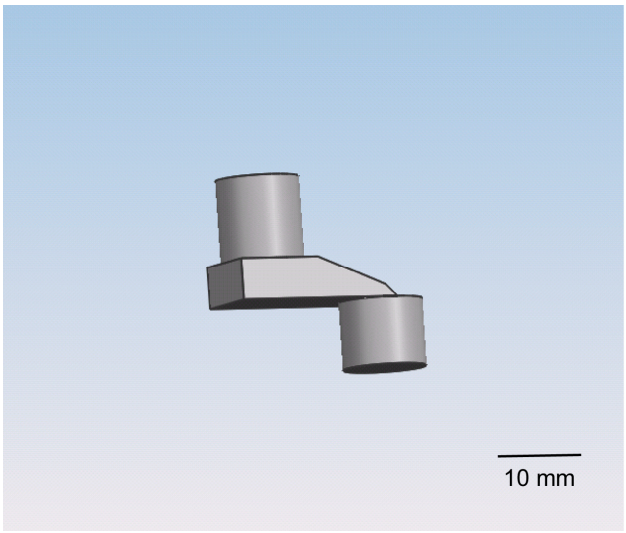

(a)

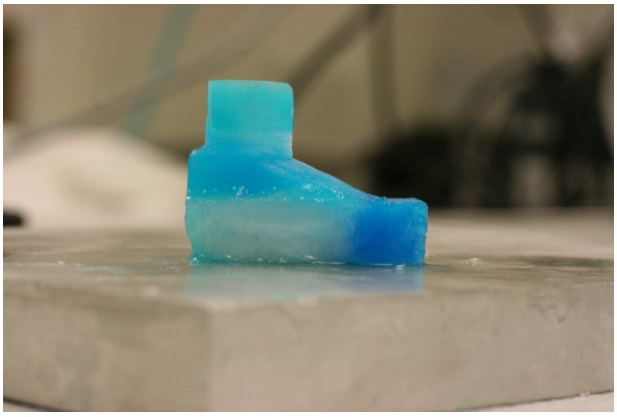

(b)

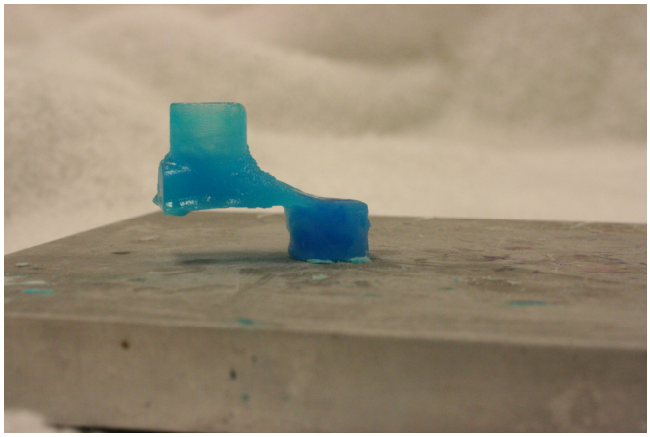

(c)

Figure 6.17. CAD model of an ice part (a), ice part before support material removal (b), and after support material removal (c)

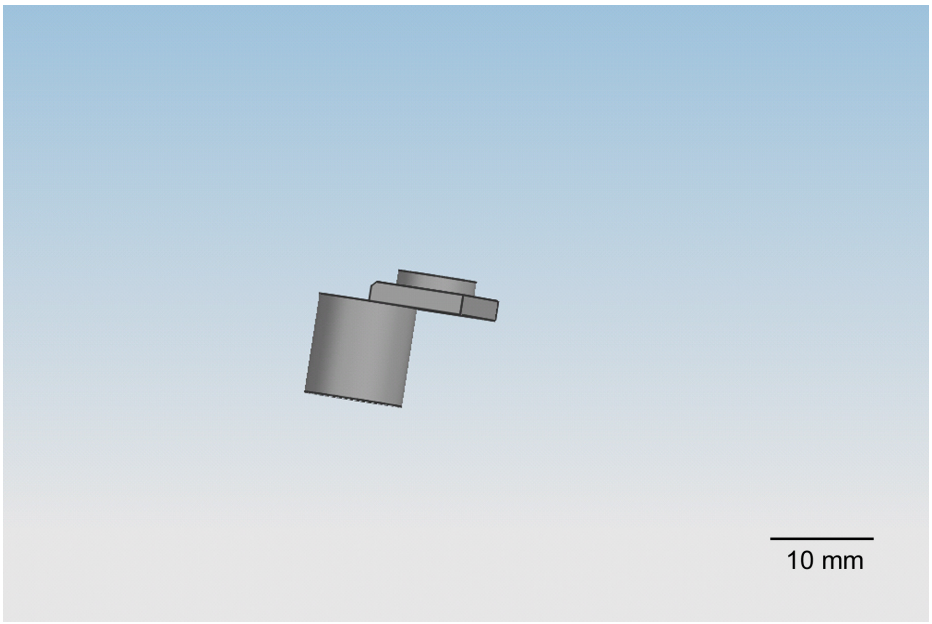

(a)

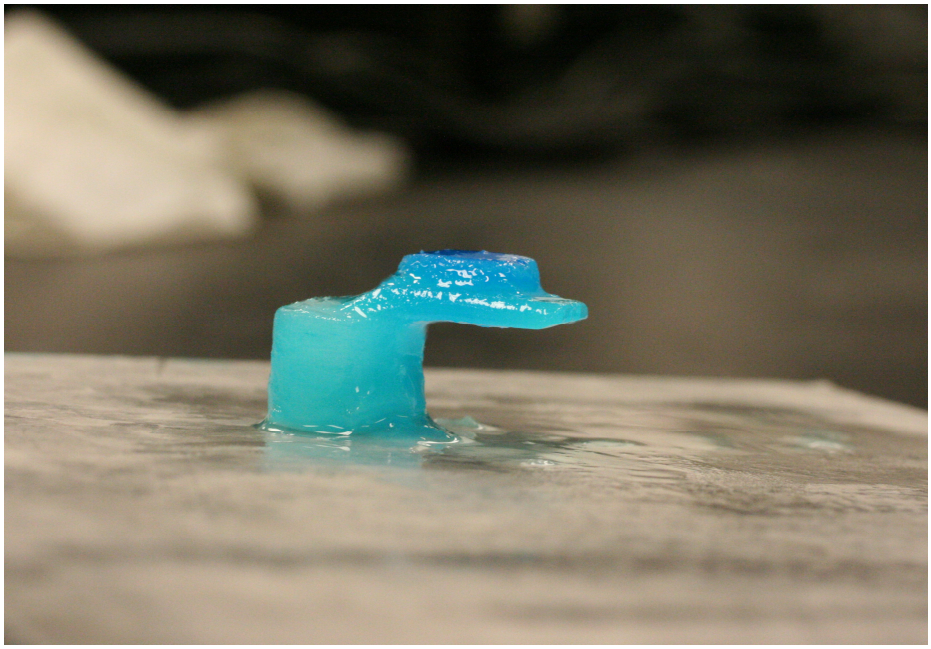

(b)

Figure 6.18. CAD model of a cantilever ice part (a) and Ice part after support material removal (b)

6.4 CONCLUDING REMARKS

Ice cylinders were fabricated to determine to what extent dimensional accuracy and surface finish can be achieved in RFP, with and without the use of support material. In the case where support material was not used in the process, and also in the case where support material was used in a -22 °C ambient, there was no significant difference in the part dimensions. The ice part dimensions in these cases were all within +/- 0.3 mm of the nominal dimensions. In the case where support material was used in the center region of a cylinder and the build temperature was -18 °C, the predicted inner diameter was smaller than predicted, by an average of 0.41 mm based on the continuous concentration model and 0.53 mm based on the discrete concentration model. Both continuous and discrete concentration models underestimate the effect of diffusion. This is probably due to these models being developed for thin wall predictions and the cylinders built in this study were solid ice parts.

7. CONCLUSIONS AND FUTURE WORK

The conclusions from this dissertation study are presented in this section. Future work that is needed to further improve the RFP process is also discussed.

7.1 CONCLUSIONS

The process parameters in the RFP process have been investigated. It has been shown how to set the values of process parameters in order to achieve desired line dimensions when fabricating parts with RFP. A suitable support material, which can now be used in RFP to create overhung areas and complex geometries, has been identified as a eutectic dextrose/water solution. Material properties of the support material have been discussed in detail, as well as the concentration criteria for removing various thicknesses of support regions in a fabricated ice part.

The temperature changes occurring during ice part fabrication by RFP have been modeled and verified with experimentally measured data. The concentration changes, which occur during the interaction of the main and support materials in liquid phase during fabrication, was predicted by using two different models. The continuous concentration model considered an infinite-source type problem which is computationally more efficient, though not a physically accurate representation of the layer-by-layer manufacture process of RFP. The discrete concentration model more accurately replicated the layer-by-layer fabrication process, but this model has a higher computation cost. Both concentration models took data as input obtained from the temperature model and predicted concentration changes that occur in the vicinity of the interface between the main and support materials. Experimentally measured height data was used as a comparison for both concentration models. The continuous concentration model was

within 5.8% of a predicted wall height dimension for ambient build temperatures ranging from -13 °C to -23.5 °C. The discrete concentration model was within 4.9 % for the predicted wall height for the same ambient temperature range.

A dimensional accuracy study was performed to simulate four different build cases. The cases where support material was not used in a -18 °C and -22 °C build ambient temperature, as well as when support material was used in a -22 °C build ambient, had an agreement to within 0.3 mm to the cylinder's nominal inner and outer diameter and height dimensions. In the case where support material was used in a -18 °C build ambient, diffusion significantly affected the inner diameter dimension where support material came into contact with water. The continuous concentration model over-estimated the impact of diffusion on the final measured dimensions by 0.41 mm, while the discrete concentration model over-estimated the inner diameter dimension by 0.53 mm. The over-estimation is most likely due to the concentration models being constructed for thin-wall cases, and the ice cylinders were solid parts constructed with 9 lines that were 1.2 mm in thickness each. Surface finish was measured on the top face of the cylinders and found to be 3.4 micron on average. The surface finish was also measured on ice surfaces where support material had been removed and the average measurement when using a planar support material area to build on was 2.6 micron, and where deposited support material was build on the average surface roughness measurement was 1.26 micron.

7.2 FUTURE WORK

Future work in the RFP study could include investigating a nozzle configuration that allows for multiple droplets to be deposited concurrently, as well as water and support material being deposited simultaneously. This would greatly decrease build time and could potentially increase the quality of the fabricated ice part in terms of both dimensional accuracy and surface roughness.

Currently the nozzle and the axes in the RFP setup are controlled by two different software controllers. Synchronizing the movement of the XY-table with the opening of the nozzle is challenging. If one software were to control both the linear axes and the nozzle, planning of the part building would be more efficient and be able to encompass greater geometries than the current system can handle. A common software, such as LabView, could be used to control the nozzles and the XY-table and another software, such as Insight, could be used for path planning of ice parts.

Controlling the ambient build temperature in a more precise manner would also benefit the RFP process. Using a different freezer to adapt to the use of a controlled temperature setting would help to ensure consistent build parameters.

RFP has already been used as a basis for a different type of freeform fabrication, which is the Freeze-form Extrusion Fabrication Process (FEF). FEF uses water as the liquid medium for a paste deposition. Using RFP as a basis for new types of freeform fabrication is another future work item to consider. RFP could potentially be used with biomaterials to create scaffold structures. The water/ice would serve as a support material and could be melted afterwards in order to have a completed intricate scaffold fabricated from biomaterials.

Three-dimensional temperature and concentration modeling would also be desirable to have. Modeling in three-dimensions would be able to better predict the concentration changes that occur during fabrication of thick-walled and solid ice parts with support.

BIBLIOGRAPHY

ANSYS Thermal Analysis Guide, 2004, ANSYS release 9.0.

Bird, R.B., Stewart, W.E., and Lightfoot, E.N., *Transport Phenomena,* 2nd Edition, John Wiley & Sons, Inc., Hoboken, NJ.

Brodkey, R. S. , 1967, *The Phenomena of Fluid Motions*, Addison-Wesley, Reading, MA.

Bryant, F. and Leu, M. C., 2004, "Study on Incorporating Support Material in Rapid Freeze Prototyping," *Proceedings of Solid Freeform Fabrication Symposium*, University of Texas at Austin, Austin, TX.

[a]Bryant, F. and Leu, M.C., 2007, "Modeling and Validation of Temperature and Concentration for Rapid Freeze Prototyping," Proceedings of Solid Freeform Fabrication Symposium, University of Texas at Austin, Austin, TX.

[b]Bryant, F., Sui, G., and Leu, M. C., 2002, "A Study on the Effects of Process Parameters in Rapid Freeze Prototyping," *Proceedings of Solid Freeform Fabrication Symposium*, University of Texas at Austin, Austin, TX.

Bryant, F., Sui, G., and Leu, M. C., 2003, "A Study on the Effects of Process Parameters in Rapid Freeze Prototyping," Rapid Prototyping Journal, Vol. 9, No. 1, pg. 19-23

Chande, T. and Mazumder, J., 1983, "Composition Control in Laser Surface Alloying," Metallurgical Transactions B, Vol. 14B, pp. 181 – 190.

Chen, T. and Zhang, Y., 2006, "Three-Dimensional Modeling of Selective Laser Sintering of Two-Component Metal Powder Layers," ASME Journal of Manufacturing Science and Engineering, Vol. 128, February 2006, pp. 299-306.

Chin, R.K., Beuth, J.L. and Amon, C.H. 2001, "Successive Deposition of Metals in Solid Freeform Fabrication Processes, Part 1: Thermomechanical Models of Layers and Droplet Columns," Journal of Manufacturing Science and Engineering, Vol. 123, pp. 623 – 631.

Chin, R.K., Beuth, J.L. and Amon, C.H. 2001, "Successive Deposition of Metals in Solid Freeform Fabrication Processes, Part 2: Thermomechanical Models of Adjacent Droplets," Journal of Manufacturing Science and Engineering, Vol. 123, pp. 632 – 638.

Crank, J., 1956, *The Mathematics of Diffusion*, Oxford at the Clarendon Press, London.

[a]Crank, J., 1984, *Free and Moving Boundary Problems*, Clarendon Press, Oxford.

Fay, J. A., 1994, *Introduction to Fluid Mechanics*, Massachusetts Institute of Technology, Cambridge, MA.

Gould, R. F., 1964, *Contact Angle, Wettability and Adhesion*, American Chemical Soceity, Washington D.C.

Jackson, R.F., Silsbee, C. G., 1922, National Bureau of Standards Scientific Papers, Number 17, Vol. 17, No. 1404.

Kar, A. and Mazumder, J., 1988, "One-dimensional Finite-Medium Diffusion Model for Extended Solid Solution in Laser Cladding of Hf on Nickel," Acta metall. , Vol. 36, pp. 701 – 712.

Leu, M. C., Zhang, W., and Sui, G., 2000, "An Experimental and Analytical Study of Ice Part Fabrication with Rapid Freeze Prototyping," Annals of the CIRP, vol. 49/1, pp. 147-150.

Leu, M. C., Liu, Q. and Bryant, F. D., 2003, "Study of Part Geometric Features and Support Materials in Rapid Freeze Prototyping," Annals of the CIRP, vol. 52/1, pp. 185 – 188.

Liu, Q. and Leu M.C., "Finite Element Analysis of Solidifying Processes in Rapid Freeze Prototyping," Proceedings of IMECE2004: ASME International Mechanical Engineering Congress, November 13-19, 2004, Anaheim, CA USA.

[a]Liu, Q. and Leu M.C., 2004, "Finite Element Analysis of Solidifying Processes in Rapid Freeze Prototyping," ASME Journal of Manufacturing Science and Engineering**,** Vol. 129, No. 4, pp. 810-820

Lunardini, V. J., 1991, *Heat Transfer with Freezing and Thawing*, Elsevier, New York

March, N.H., and Tosi, M.P., 2002, *Introduction to Liquid State Physics*, World Scientific, Singapore

Munson, B. R., Young, D. F., and Okiishi, T. H., 1994, *Fundamentals of Fluid Mechanics*, John Wiley & Sons, Inc., New York.

Ozisik, M. N., 1985, *Heat Transfer: A Basic Approach,* McGraw-Hill, Inc., New York

Rosenthal, D., 1946, "The Theory of Moving Sources of Heat and Its Application to Metal Treatments," Transactions of ASME, vol. 68, pp. 849-866.

Stephan, H. and Stephan, T., "Solubilities of Inorganic and Organic Compounds," Vol. 1, Pergamon Press, New York. 1963. pg. 108.

Sui, G. and Leu, M.C., 2003, "Thermal Analysis of Ice Wall Built by Rapid Freeze Prototyping," ASME Journal of Manufacturing Science and Engineering, Vol. 125, No. 4, November 2003, pp. 824-834.

[a]Sui, G., Leu M., 2002, "Investigation of Layer Thickness and Surface Roughness in Rapid Freeze Prototyping," ASME Journal of Manufacturing Science and Engineering, Vol. 125, No. 3, pp 556-563.

[b]Sui, G., 2002, "*Modeling and Analysis of Rapid Freeze Prototyping," PhD dissertation, University of Missouri-Rolla, Rolla, MO.*

The Lee Company webpage (http://www.theleeco.com/EFSWEB/2142.htm), Last viewed: August 25, 2008.

Vasinonta, A., Beuth, J.L. and Griffith, M.L., 2001, "A Process Map for Consistent Build Conditoins in the Solid Freeform Fabrication of Thin-Walled Structures," Journal of Manufacturing Science and Engineering, Vol. 123, pp. 615-622.

Walas, S. M., 1985, *Phase Equilibria in Chemical Engineering*, Butterworth-Heinemann, Boston.

Zhang, W., Leu, M.C., Ji Z. and Yan Y., 1999, "Rapid Freezing Prototyping with Water," Materials and Design, vol. 20, pp. 139-145.

VITA

Frances Denise Bryant nee Hilding was born on July 28, 1974 in Weisbaden, Germany. She finished her primary and secondary education in May 1992 from the Fort Osage school district in Independence, MO. She then attended The University of Missouri-Rolla and received a Bachelor of Science in Mechanical Engineering in December 1996. Following graduation, Mrs. Bryant was employed by Emerson Electric in St. Louis, MO. During her employment, Mrs. Bryant attended the University of Missouri-Rolla's Engineering Extension Center in St. Louis during the evenings and obtained a Master of Science degree in Mechanical Engineering in December 2000.

In 2002, Mrs. Bryant returned to the University of Missouri-Rolla to work on her Ph.D. degree. At various times throughout working on her Ph.D., Mrs. Bryant was a U.S. Department of Education (GAANN) Fellow, a research assistant, a graduate teaching assistant and a lecturer. In January 2008, The University of Missouri-Rolla was renamed to The Missouri University of Science and Technology. She received her Ph.D. from The Missouri University of Science and Technology in December 2008.